

# RobustECD: Enhancement of Network Structure for Robust Community Detection

Jiajun Zhou, Zhi Chen, Min Du, Lihong Chen, Shanqing Yu,  
Guanrong Chen, *Fellow, IEEE*, and Qi Xuan, *Member, IEEE*

**Abstract**—Community detection, which focuses on clustering vertex interactions, plays a significant role in network analysis. However, it also faces numerous challenges like missing data and adversarial attack. How to further improve the performance and robustness of community detection for real-world networks has raised great concerns. In this paper, we explore *robust community detection* by enhancing network structure, with two generic algorithms presented: one is named *robust community detection via genetic algorithm* (*RobustECD-GA*), in which the modularity and the number of clusters are combined in a fitness function to find the optimal structure enhancement scheme; the other is called *robust community detection via similarity ensemble* (*RobustECD-SE*), integrating multiple information of community structures captured by various vertex similarities, which scales well on large-scale networks. Comprehensive experiments on real-world networks demonstrate, by comparing with two traditional enhancement strategies, that the new methods help six representative community detection algorithms achieve more significant performance improvement. Moreover, experiments on the corresponding adversarial networks indicate that the new methods could also optimize the network structure to a certain extent, achieving stronger robustness against adversarial attack. The source code of this paper is released on <https://github.com/jjzhou012/RobustECD>.

**Index Terms**—Community detection, Genetic algorithm, Vertex similarity, Structure enhancement, Adversarial attack

## 1 INTRODUCTION

COMMUNITY detection, or network clustering, which aims to identify groups of interacting vertices in a network in term of their structural properties, has recently attracted considerable attention from different fields like sociology, biology and computer science [1], [2]. Community structure is of ultra importance in network analysis. Typically in networks, vertices are organized into groups, called *communities*, *clusters* or *modules*, with dense connections within groups and sparse connections between them. For instance, in co-author networks, communities are formed by scientists with similar research interests in close fields; in social networks like Facebook, they can represent people focusing on similar topics. Many recent researches suggest that network properties at the community level are quite different from those at the global level, and thus ignoring community structure may miss many interesting features [3]. In fact, identifying communities in networks has played a significant role in exploiting essential network structures.

Until now, a large number of techniques have been developed to detect community structures in networks. However, despite the advance of various community detection methods, from spectral method, label propagation to deep learning, their capability to discover the true community

structure faces numerous challenges, since these approaches strongly rely on the topological structure of the underlying network, which is vulnerable in real-world scenarios.

First, missing data and adversarial noise seriously affect the performance of community detection algorithms. Real-world networks are often flawed in integrity and suffer from missing data, since not all real-world relationships are reflected in a single network. For instance, users in social networks like Twitter seldom follow all their friends in activities. Moreover, missing data also occurs when crawling datasets from online networks with privacy restrictions. On the other hand, the accuracy of a network is very likely to be questioned when the information encoded in the network topology is perturbed by artificial noise, especially when the network suffers from adversarial attacks, which leads to the degradation of the performance of many network analysis methods. In particular, adversarial attacks against community detection aim to hide target communities or sensitive edges [4], [5], and finally generate specific adversarial networks, which can strongly impact the performance of detection algorithms. Existing community detection methods rarely consider missing data and adversarial noise in networks, increasing the risk to obtain wrong community structures.

Another challenge is the lack of a consensus on the formal definition of a network community structure [6]. Currently, there are no universal standards for the definition of community, and a large number of detection algorithms based on different technologies and ideas have been proposed, which led to a quality discrepancy among different results. Moreover, modularity optimization in community detection has a resolution limit [7]. Clusters consisting of a number of vertices smaller than a threshold would not be detected because these clusters tend to merge into larger

- J. Zhou, L. Chen, S. Yu, and Q. Xuan are with the Institute of Cyberspace Security, College of Information Engineering, Zhejiang University of Technology, Hangzhou 310023, China. E-mail: {jjzhou012@163.com, {yushanqing, 2111803032, xuanqi}@zjut.edu.cn).
- Z. Chen and M. Du are with the Department of Electrical Engineering and Computer Sciences, University of California, Berkeley, CA 94720, USA. E-mail: {zhichen98, min.du}@berkeley.edu.
- G. Chen is with the Department of Electrical Engineering, City University of Hong Kong, Hong Kong SAR, China. E-mail: eegchen@cityu.edu.hk.
- J. Zhou and Z. Chen make equal contribution.
- Corresponding author: Qi Xuan.

ones by modularity optimization. Large, but locally sparse communities probably tend to be subdivided into smaller ones during community partition.

It is believed that such challenges are mostly from unstable network structures. Networks with sparse community structures are vulnerable to adversarial attacks which can destroy network structures, leading to community detection deception. Generally, communities with weak structures could be absorbed from the outside or disintegrated from the inside of the network. Enhancing the network structure and improving the robustness of the network could be an effective way to address these challenges. In this paper, we explore *robust community detection* by enhancing network structures, and develop two algorithms. A heuristic idea comes from the fact that community structures show a high connection density of intra-communities and a sparse one of inter-communities. Agglomerating the intra-communities by adding edges between internal vertices and dividing the inter-communities by removing edges between communities, therefore, can strengthen the community structure in a network. It's a natural reversal of the studies about community detection deception in [4], [5] where they are proposed to weaken community structures via intra-community edge deletion and inter-community edge addition. Another idea for robust community detection is to enhance network structure with edge prediction, of which the task is to complement missing edges or predict future edges between pairwise vertices based on the current network structure. The vertex similarity indices can be used to guide network structure optimization, according to the following two assumptions: 1) vertices in the same community are aggregated based on their high similarity; 2) a larger similarity of pairwise vertices leads to a higher likelihood of edges between them [8]. The main contributions of our work are summarized as follows:

- First, we study the *Robust Community Detection via network structure Enhancement (RobustECD)*, which can improve the performance of existing detection algorithms. To the best of our knowledge, our work is the first for enhancing community detection in both real-world networks and adversarial networks.
- Second, we develop two generic enhancement algorithms, namely *robust community detection via genetic algorithm (RobustECD-GA)* and *robust community detection via similarity ensemble (RobustECD-SE)*. Experimental results in six real-world networks demonstrate the superiority of our methods in helping six community detection algorithms to achieve significant improvement of performances.
- Third, we test our enhancement algorithms on four adversarial networks, the results show that both *RobustECD-GA* and *RobustECD-SE* can optimize the network structure to a certain extent, and achieve robust community detection against adversarial attack.
- Finally, our methods could alleviate the resolution limit in modularity optimization, and help various community detection algorithms to achieve consensus, i.e., getting more consistent partitions.

The rest of the paper is organized as follows. First, in Sec. 2, we review the related works. Then, in Sec. 3, we describe our approaches in detail. Thereafter, we present extensive

experiments in Sec. 4, with a series of discussions. Finally, we conclude the paper and outline future work in Sec. 5.

## 2 RELATED WORK

### 2.1 Community Detection

Community detection strives to identify groups of interacting vertices by maximizing cluster quality measures such as modularity [9] and normalized mutual information [10]. The literature [11] has provided comprehensive reviews on community detection. For community detection in undirected networks, widely used methods concentrate on agglomerative [12], divisive [3], [13], hierarchical [13], [14], spectral [15], [16], random walk [17], [18], label propagation [19], [20], high-order [21] and deep learning [22], [23] methods.

### 2.2 Traditional Enhancement of Community Detection

Due to the deficiency of many detection methods, how to improve their performance in complicated real applications has become an important issue. In this paper, we focus on the problem of enhancing existing community detection methods. Existing traditional enhancement approaches suggest preprocessing networks via weighting or rewiring. Meo et al. [24] introduced a measure of  $\kappa$ -path edge centrality and proposed a weighting algorithm called WERW-Kpath to effectively compute the centrality as edge weight, which is better for community detection. Sun [25] weighted networks via a series of edge centrality indices and detected communities in the weighted network using a function that considers both links and link weights. Lai et al. [26] considered random walk for simulation on dynamic processes, and applied it to enhance modularity optimization, based on the intuition that pairwise vertices in the same community have similar dynamic patterns. Interestingly, Li et al. [27] considered motif-aware community detection which achieves community partition using motif information in networks, and proposed an edge enhancement approach called Edmot. Their method transfers the network into motif-based hypergraph and partitions it into modules, and then a new edge set is constructed to enhance the connectivity structure of the original network by fully connecting all modules. Lancichinetti et al. [28] proposed consensus clustering algorithm, which combines the information of different outputs to obtain a more representative partition, to analyze the time evolution of clusters in dynamics networks. Dahlin et al. [29] proposed the ensemble cluster that combines the ensemble method with clustering, and improve community detection by aggregating multiple runs of algorithms. On the other hand, model-based methods tend to integrate the enhancement into the whole community detection procedure. For example, He et al. [30] provided a framework to enhance the ability of non-negative matrix factorization (NMF) models to detect communities, which uses the NMF method to train a stochastic model constrained by vertex similarity.

### 2.3 Adversarial Attack on Community Detection

In this paper, since some experiments are conducted on networks with adversarial noise which are generated via adversarial attack [31], we briefly review the research on adversarial attack for community detection. Waniek et al. [32] proposed a simple heuristic method deployed

TABLE 1  
Main notations used in this paper.

Symbol	Description
$\mathcal{G}$	The target network
$\mathcal{V}, \mathcal{E}, \mathcal{M}$	Sets of vertices, edges, communities in $\mathcal{G}$
$n, m$	Numbers of vertices, edges in $\mathcal{G}$
$v, e$	Vertex, edge in $\mathcal{G}$
$S$	The studied community detection algorithm
$\mathcal{M}_S, \phi_S$	Set/Number of communities found by $S$ in $\mathcal{G}$
$\mathcal{M}_{real}, \phi_{real}$	Set/Number of the ground-truth communities in $\mathcal{G}$
$\mathcal{E}_{add}, \mathcal{E}_{del}$	The schemes of edge addition/deletion
$\beta_a, \beta_d$	budget of edge addition/deletion
$\mathcal{Q}$	Modularity
$\phi_p$	Size of population
$T_{ga}$	Number of iterations
$\mathcal{G}_{co}, \mathcal{A}_{co}$	Co-occurrence network and its adjacency matrix
$\mathcal{T}$	Threshold of prune in $\mathcal{G}_{co}$
$\mathcal{H}$	Similarity metric (or similarity matrix)
$\mathcal{G}_{co}^T$	Co-occurrence graph pruned with threshold $\mathcal{T}$
$\mathcal{M}^T$	Community partition in pruned graph $\mathcal{G}_{co}^T$
$c, C$	Consensus of a cluster/partition

by intra-community edge deletion and inter-community edge addition, and introduced a measure of concealment to express how well a community is hidden. Fionda et al. [5] introduced and formalized the community deception problem, and proposed a community deception algorithm based on safeness, which achieves a success in hiding a target community. Chen et al. [4] proposed an effective evolutionary computation strategy, namely genetic algorithm (GA)-based  $\mathcal{Q}$ -Attack, to achieve deception by negligibly rewiring networks. Li et al. [33] proposed an end-to-end graph neural framework that combines graph generator and graph partitioner, and achieved the generation of adversarial examples of high quality and generalization.

### 3 METHODOLOGY

In this section, we first formulate the problem of community detection, and then present two enhancement strategies. The main notations used in this paper are listed in TABLE 1.

#### 3.1 Problem Formulation

Assume that an undirected and unweighted network is represented by a graph  $\mathcal{G} = (\mathcal{V}, \mathcal{E})$ , which consists of a vertex set  $\mathcal{V} = \{v_i \mid i = 1, \dots, n\}$  and an edge set  $\mathcal{E} = \{e_i \mid i = 1, \dots, m\}$ . The topological structure of graph  $\mathcal{G}$  is represented by an  $n \times n$  adjacency matrix  $\mathcal{A}$  with  $\mathcal{A}_{ij} = 1$  if  $(v_i, v_j) \in \mathcal{E}$  and  $\mathcal{A}_{ij} = 0$  otherwise. The nonexistent edge set  $\bar{\mathcal{E}}$  is represented by  $\{(v_i, v_j) \mid \mathcal{A}_{ij} = 0; i \neq j\}$ . The task of community detection in a network is to find a vertex partition  $\mathcal{M} = \{\mathcal{M}_i \mid i = 1, \dots, k\}$ , with  $\bigcup \mathcal{M}_i = \mathcal{V}$  and  $\mathcal{M}_i \cap \mathcal{M}_j = \emptyset$  for  $i \neq j$ , where set  $\mathcal{M}_i$  is called a *community*. The ground-truth community partition of the network is denoted as  $\mathcal{M}_{real}$ . Note that the community overlapping problem will not be considered in this paper.

We further explore the network structure enhancement from heuristic and optimized approaches. In the enhancement scenario, a network will be rewired via edge modification, during which the edges removed from network are sampled from the candidate set  $\mathcal{E}_{del}^c$ , while the edges added to the network are sampled from the candidate pairwise

vertices set  $\mathcal{E}_{add}^c$ . The construction of candidate sets varies for different methods, as further discussed below.

For a network  $\mathcal{G}$ , one can get the set of edges added/removed from  $\mathcal{G}$  via sampling from the candidate sets:

$$\begin{aligned} \mathcal{E}_{del} &= \{\tilde{e}_i \mid i = 1, \dots, \lceil m \cdot \beta_d \rceil\} \subset \mathcal{E}_{del}^c, \\ \mathcal{E}_{add} &= \{\tilde{e}_i \mid i = 1, \dots, \lceil m \cdot \beta_a \rceil\} \subset \mathcal{E}_{add}^c, \end{aligned} \quad (1)$$

where  $\beta_a, \beta_d$  are the budget of edge addition/deletion and  $\lceil x \rceil = \text{ceil}(x)$ . Then, based on the modification scheme  $\mathcal{E}_{mod} = (\mathcal{E}_{add}, \mathcal{E}_{del})$ , the connectivity structure of the original network is optimized to generate a rewired network:

$$\mathcal{G}^* = (\mathcal{V}, \mathcal{E}^*) \quad \text{with } \mathcal{E}^* = \mathcal{E} \cup \mathcal{E}_{add} \setminus \mathcal{E}_{del}. \quad (2)$$

For the rewired networks obtained via enhancement, we expect that the community detection methods perform significantly better and the new partition  $\mathcal{M}^*$  is closer to the ground-truth communities, i.e., there is a significant improvement in evaluation metrics after assigning  $\mathcal{M}^*$  to  $\mathcal{G}$ .

#### 3.2 Modularity-Based Structure Enhancement

Previous works [4], [5], [32] have shown that intra-community edge deletion and inter-community edge addition can facilitate the deployment of community deception attacks. By contrast, it is natural that agglomerating the intra-communities by adding edges between internal vertices and dividing the inter-communities by removing edges between communities, i.e. intra-community edge addition and inter-community edge deletion, can strengthen the community structures in a network. Meanwhile, the resolution limitation problem that cannot be neglected requires the proposed approach to be capable of combining these four basic community edge modifications organically. Therefore, based on modularity, we propose the first method, named *robust community detection via genetic algorithm (RobustECD-GA)*, which aims to enhance community structure via adaptable community edge rewiring. The schematic depiction of *RobustECD-GA* is shown in Fig. 1.

##### 3.2.1 Network Rewiring

Given a network  $\mathcal{G}$ , a community edge optimization strategy requires knowledge of the community structure to pick the optimal edge modification schemes and thus depends on the prior community detection algorithm  $\mathcal{S}$  that generates the estimated partition  $\mathcal{M}_S = \{\mathcal{M}_i \mid i = 1, \dots, k\}$ . For arbitrary pairwise vertices  $(v_i, v_j)$ , the candidate sets of four basic community edge modifications are represented as follows:

$$\begin{aligned} \mathcal{E}_{intra-add}^c &= \{(v_i, v_j) \mid v_i, v_j \in \mathcal{M}_i, \mathcal{A}_{ij} = 0\}, \\ \mathcal{E}_{intra-del}^c &= \{(v_i, v_j) \mid v_i, v_j \in \mathcal{M}_i, \mathcal{A}_{ij} = 1\}, \\ \mathcal{E}_{inter-add}^c &= \{(v_i, v_j) \mid v_i \in \mathcal{M}_i, v_j \in \mathcal{M}_j, \mathcal{A}_{ij} = 0\}, \\ \mathcal{E}_{inter-del}^c &= \{(v_i, v_j) \mid v_i \in \mathcal{M}_i, v_j \in \mathcal{M}_j, \mathcal{A}_{ij} = 1\}, \end{aligned} \quad (3)$$

where  $\mathcal{M}_i, \mathcal{M}_j \in \mathcal{M}_S$ ,  $\mathcal{E}_{intra-del}^c \cup \mathcal{E}_{inter-del}^c = \mathcal{E}$  and  $\mathcal{E}_{intra-add}^c \cup \mathcal{E}_{inter-add}^c = \bar{\mathcal{E}}$ .

The adaptable community edge rewiring consists of two parts, one is the required intra-community edge addition and inter-community edge deletion, and the other is an optional part that depends on the comparison between the number

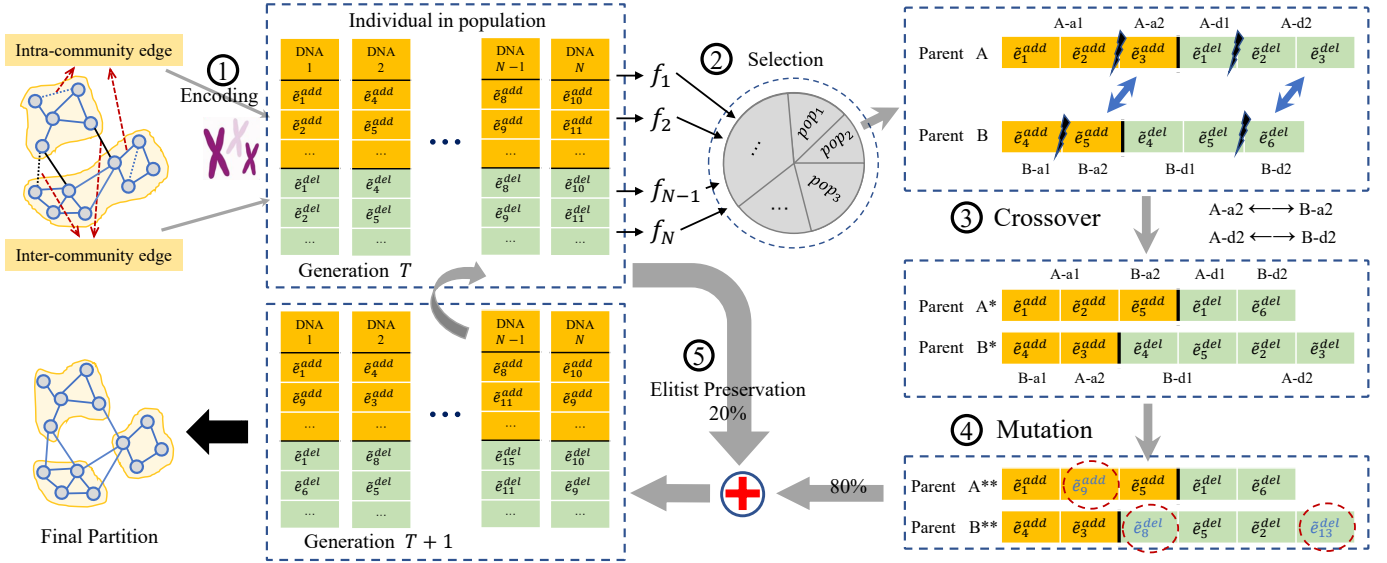


Fig. 1. Schematic depiction of *RobustECD-GA*. The workflow of evolution iteration proceeds as follows: 1) chromosome encoding for population initialization; 2) fitness calculation and individual selection; 3) chromosome crossover; 4) chromosome mutation; 5) elitist preservation.

of communities in the estimated partition and the one in the ground truth:

$$\mathcal{E}_{mod} = \begin{cases} (\mathcal{E}_{add} \subset \bar{\mathcal{E}}, \mathcal{E}_{del} \subset \mathcal{E}_{inter-del}^c) & \phi_S > \phi_{real} \\ (\mathcal{E}_{add} \subset \mathcal{E}_{intra-add}^c, \mathcal{E}_{del} \subset \mathcal{E}) & \phi_S < \phi_{real} \\ (\mathcal{E}_{add} \subset \mathcal{E}_{intra-add}^c, \mathcal{E}_{del} \subset \mathcal{E}_{inter-del}^c) & \phi_S = \phi_{real} \end{cases} \quad (4)$$

where  $\phi_{real}$  is the number of the ground-truth communities and  $\phi_S$  is the number of communities in the estimated partition  $\mathcal{M}_S$ . Eq (4) lists three scenarios caused by resolution limit during initialization of edge modification:

- When  $\phi_S > \phi_{real}$ , there is a relatively high resolution, and large but locally sparse communities tend to be subdivided into smaller fragments. Ideally, extra inter-community edge addition is conducive to aggregate those fragments into integrate communities;
- When  $\phi_S < \phi_{real}$ , there is a relatively low resolution, and clusters consisting of a number of vertices smaller than a threshold tend to merge into larger ones. Ideally, extra intra-community edge deletion is conducive to subdivide large clusters;
- When  $\phi_S = \phi_{real}$ , there is a relatively suitable resolution. Both the inter-community edge addition and intra-community edge deletion are inoperative.

Notably, the aforementioned adaptable community edge rewiring requires knowledge of the ground-truth community (i.e.,  $\mathcal{M}_{real}$  and  $\phi_{real}$ ). When it comes to the dilemma that ground-truth communities are not available, the rewiring mechanism preserves only the required part, i.e., intra-community edge addition and inter-community edge deletion.

### 3.2.2 Evolutionary Optimization

We use the genetic algorithm (GA) due to its good performance in solving combinatorial optimization problems. Specifically, we design the encoding scheme of chromosome and the function of fitness as follows.

- **Chromosome.** Chromosome represents an edge modification scheme  $\mathcal{E}_{mod}$ , consisting of two parts:  $\mathcal{E}_{add}$

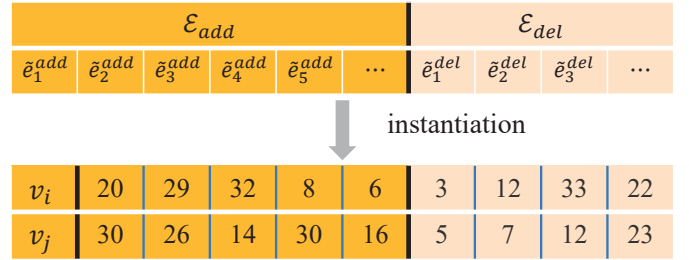


Fig. 2. The diagram of chromosome in *RobustECD-GA*. It consists of two parts including edge addition segment  $\mathcal{E}_{add}$  and edge deletion segment  $\mathcal{E}_{del}$ . The instance of chromosome is initialized in the experiment for Karate dataset, with an edge addition segment of length 5 and an edge deletion segment of length 4.

and  $\mathcal{E}_{del}$ , where a gene denotes an edge modification operation, including edge addition or deletion. The diagram of chromosome is shown in Fig. 2.

- **Fitness.** Modularity [9] has been widely applied in community detection task and is an effective evaluation metric to assess the quality of network partition (more details please refer to Sec. 4.2). Here, the fitness is defined as:

$$f = |Q|/e^{|\phi_S - \phi_{real}|}, \quad (5)$$

where  $Q$  is the modularity of the partition for the target network and  $e$  is Euler's number. Denominator  $e^{|\phi_S - \phi_{real}|}$  is typically chosen to impose a penalty on the size of resolution. Modularity is divided by a large penalty term which is no less than  $e$  when  $\phi_S \neq \phi_{real}$ , and the fitness function degenerates to modularity when  $\phi_S = \phi_{real}$  or no access to the ground-truth community. Individuals with larger modularity and more accurate partition generally have larger fitness.

The procedure of *RobustECD-GA* is shown in Algorithm 1. As mentioned above, *RobustECD-GA* requires the knowledge of the community structure, which guides the edge modification. We feed the target network  $\mathcal{G}$  into community detection algorithm  $\mathcal{S}$  to generate a general community partition  $\mathcal{M}_S$  and then construct the candidate edge sets (line 1).

During **initialization**, a parental generation  $\mathcal{P} =$

**Algorithm 1: RobustECD-GA**


---

**Input:** Target network  $\mathcal{G}$ , community detection algorithm  $\mathcal{S}$ , parameter for GA( $\phi_p, \mathcal{P}_c, \mathcal{P}_m, \mathcal{P}_e, \mathcal{T}_{ga}$ ), budget  $\beta_a, \beta_d$ .

**Output:** New community partition  $\mathcal{M}^*$

- 1  $\mathcal{M}_S \leftarrow \text{detectCommunity}(\mathcal{S}, \mathcal{G})$ ;
- 2  $\mathcal{P}, \mathcal{F} \leftarrow \text{initializePop}(\mathcal{G}, \mathcal{M}_S, \phi_p, \beta_a, \beta_d)$ ;
- 3 Initialize current generation  $i = 0$ ;
- 4 **while**  $i < \mathcal{T}_{ga}$  **do**
- 5      $\mathcal{P}_{elitist} \leftarrow \text{retainElitist}(\mathcal{F}, \mathcal{P}, \mathcal{P}_e)$ ;
- 6      $\mathcal{P}_{select} \leftarrow \text{selection}(\mathcal{F}, \mathcal{P})$ ;
- 7      $\mathcal{P}_{crossover} \leftarrow \text{crossover}(\mathcal{P}_{select}, \mathcal{P}_c)$ ;
- 8      $\mathcal{P}_{mutate} \leftarrow \text{mutation}(\mathcal{P}_{crossover}, \mathcal{P}_m, \mathcal{M}_S)$ ;
- 9      $\mathcal{F} \leftarrow \text{getFitness}(\mathcal{G}, \mathcal{S}, \mathcal{P}_{mutate})$ ;
- 10     $\mathcal{P} \leftarrow \text{getNextGeneration}(\mathcal{P}_{mutate}, \mathcal{P}_{elitist})$
- 11 Get the individual with highest fitness from the last population:  $\mathcal{E}_{mod} \leftarrow \text{getBestIndividual}(\mathcal{F}, \mathcal{P})$ ;
- 12 Rewire the original network to obtain  $\mathcal{G}^*$  via Eq. (2) ;
- 13 Feed  $\mathcal{G}^*$  into  $\mathcal{S}$  to generate new community partition:  $\mathcal{M}^* \leftarrow \text{detectCommunity}(\mathcal{S}, \mathcal{G}^*)$  .;
- 14 **end** ;
- 15 **return**  $\mathcal{M}^*$ ;

---

**Algorithm 2: RobustECD-SE**


---

**Input:** Target network  $\mathcal{G}$ , community detection algorithm  $\mathcal{S}$ , budget  $\beta_a$ .

**Output:** New community structure  $\mathcal{M}^*$

- 1 Compute similarity indices listed in TABLE 2:  $\{\mathcal{H}_{CN}, \dots, \mathcal{H}_{RWR}\} \leftarrow \text{computeSimilarity}(\mathcal{G})$ ;
- 2 Obtain rewire schemes via sampling:  $\{\mathcal{E}_{mod}^1, \dots\} \leftarrow \text{sample}(\mathcal{G}, \beta_a, \{\mathcal{H}_{CN}, \dots, \mathcal{H}_{RWR}\})$ ;
- 3 Update graph via network rewiring:  $\{\mathcal{G}_1^*, \dots\} \leftarrow \text{rewire}(\mathcal{G}, \{\mathcal{E}_{mod}^1, \dots\})$ ;
- 4 Obtain multiple partitions via community detection:  $\{\mathcal{M}_1^*, \dots\} \leftarrow \text{detectCommunity}(\mathcal{S}, \{\mathcal{G}_1^*, \dots\})$ ;
- 5 Get co-occurrence network from multiple partitions:  $\mathcal{G}_{co}, \mathcal{A}_{co} \leftarrow \text{getCoNetwork}(\{\mathcal{M}_1^*, \dots\})$ ;
- 6 Threshold selection:  $\mathcal{T}, \mathcal{M}_{core}^T \leftarrow \text{getOptimalThreshold}(\mathcal{G}_{co})$ ;
- 7 Get the final partition by assigning isolated vertices to core communities:  $\mathcal{M}^* \leftarrow \text{getFinalPartition}(\mathcal{M}_{core}^T, \{\mathcal{H}_{CN}, \dots, \mathcal{H}_{RWR}\})$ ;
- 8 **end** ;
- 9 **return**  $\mathcal{M}^*$ ;

---

TABLE 2

Summary of similarity indices used in this paper.  $\mathcal{H}(i, j)$  is the similarity score of pairwise vertices  $(v_i, v_j)$ ,  $\Gamma(i)$  is the 1-hop neighbors of  $v_i$ ,  $g(\cdot)$  is the nonnegative function under the given network,  $\gamma$  is a decaying factor between 0 and 1,  $\eta$  is a positive constant/function of  $\gamma$ .

Order	Category	Form	Used in paper
First	Local	$\mathcal{H}(i, j) =  \Gamma(i) \cap \Gamma(j)  \cdot g(i, j)$	Common Neighbors (CN) [8] Salton [34], Jaccard [35] Hub Promoted Index (HPI) [36]
Second	Local	$\mathcal{H}(i, j) = \sum_{z \in \Gamma(i) \cap \Gamma(j)} g(z)$	Adamic-Adar Index (AA) [37] Resource Allocation Index (RA) [38]
High	Quasi-local, Global	$\mathcal{H}(i, j) = \eta \sum_{l=1}^{\infty} \gamma^l g(i, j, l)$ [39]	Local Path Index (LP) [40] Random Walk with Restart (RWR) [41]

$\{\mathcal{E}_{mod}^i \mid i = 1, \dots, \phi_p\}$  is randomly generated with a population size  $\phi_p$  and each individual  $\mathcal{E}_{mod}^i$  in the population has an

unfixed size, i.e., the quantity of modified edges is not fixed for each initial modification scheme (line 2). During **selection**, the operation is conducted on *roulette*, which means that the probability for an individual to be selected is proportional to its fitness (line 6). **Crossover** is the process of combining the parental generation to generate new schemes and we apply *multi-point crossover* to swap gene segments between two parental chromosomes with a crossover rate  $\mathcal{P}_c$  (line 7). **Mutation** prevents the algorithm from falling into local optimization. We traverse each gene in the chromosome and conduct the mutation operation with a mutation rate  $\mathcal{P}_m$  (line 8). In so doing, we randomly replace the edge modification operation  $\tilde{e}^{add}$  or  $\tilde{e}^{del}$  with another one. Finally, **elitist preservation** is applied to retain excellent individuals, which refer to modification schemes with higher fitness. In particular, we retain excellent individuals by replacing the worst 20% of the offspring with the best 20% of the parents (line 5). Evolution is a process of iteration and we set the number of iterations  $\mathcal{T}_{ga}$  as the evolutionary generation. The evolutionary optimization stops when it is convergent or this condition is satisfied.

**3.3 Similarity-Based Structure Enhancement**

Empirically, vertices in the same community is aggregated due to their high similarity. Vertex similarity can be defined as the number of common features that a pair of vertices share [42]. Previous works [8], [39] have shown that local, global and random-walk-based similarity indices perform excellently in capturing network structure features, and further unified them into three general forms of heuristics according to the subgraph involved in the similarity calculation, as summarized in TABLE 2 and Appendix A.4. Therefore, we adopt the heuristics to aggregate those vertices of high similarity, i.e., considering the vertex similarity indices as the guidance of edge modification. Based on this, we propose the second method, named *robust community detection via similarity ensemble (RobustECD-SE)*, which rewires a network via multiple similarity indices and aggregates corresponding community partitions to generate more accurate community structures. The schematic depiction of *RobustECD-SE* is shown in Fig. 3, and the procedure of *RobustECD-SE* is shown in Algorithm 2.

**3.3.1 Network Rewiring**

In *RobustECD-SE*, the similarity rewiring is a modification of network structure at the global level, so that the candidate set of edge modification is defined as  $\mathcal{E}_{add}^c = \bar{\mathcal{E}}$ . Note that only edge addition is considered in *RobustECD-SE* and edge deletion is neglected for several reasons: 1) slight improvement of performance; 2) extra time consumption, as further discussed in Appendix A.1.

Given a target network  $\mathcal{G}$ , the similarity matrix  $\mathcal{H}$ , which consists of similarity scores of arbitrary pairwise vertices, can be directly calculated (line 1). During **similarity rewiring**, we first assign all entries in  $\mathcal{E}_{add}^c$  with relative weights that are associate with the vertex similarity scores. And we get the  $\mathcal{E}_{add}$ , the set of edges added to  $\mathcal{G}$ , via weighted random sampling from  $\mathcal{E}_{add}^c$  with a budget of  $\beta_a$ , which means that the probability for an entry in  $\mathcal{E}_{add}^c$  to be selected is proportional to its similarity score  $\mathcal{H}_{ij}$  (line 2). After edge sampling, we update network via Eq.(2) (line 3).

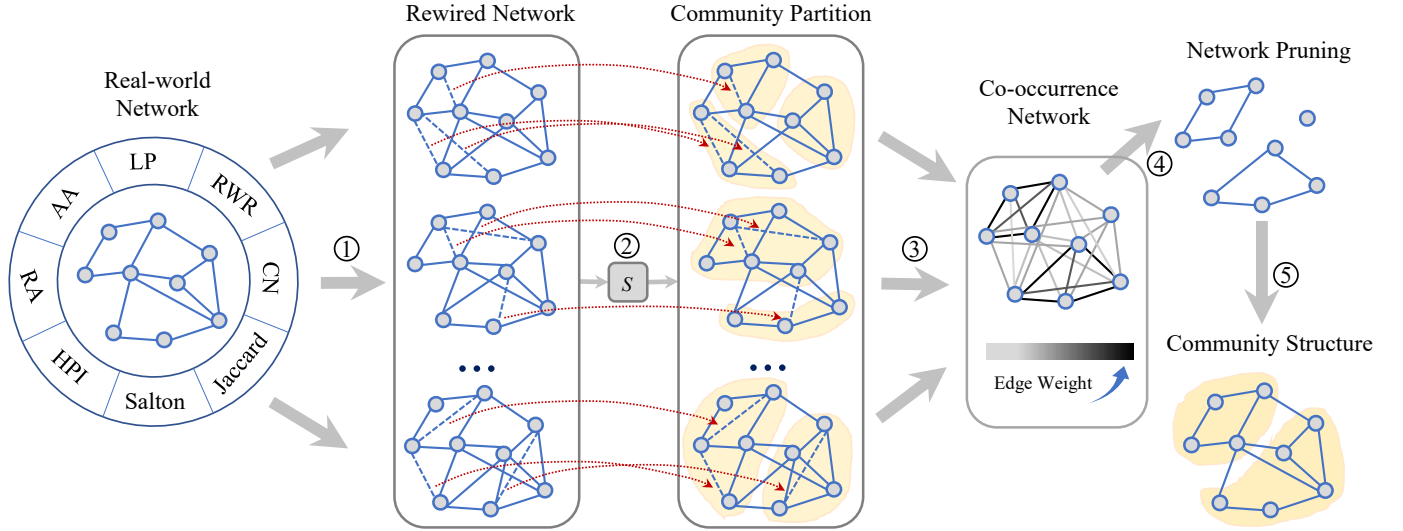


Fig. 3. Schematic depiction of *RobustECD-SE*. The complete workflow proceeds as follows: 1) similarity rewiring to generate rewired networks; 2) community detection to generate community partitions; 3) partition ensemble to generate co-occurrence network; 4) network pruning to identify core communities; 5) isolated vertices reassignment to get final community structure.

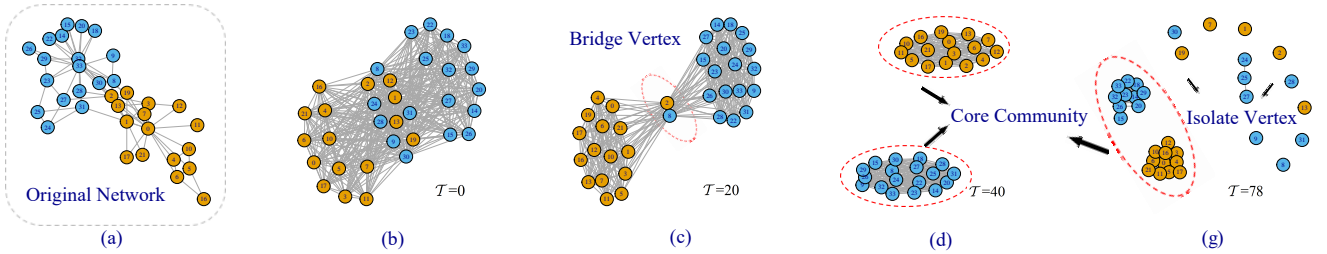


Fig. 4. Visualization of network pruning in the co-occurrence network of Karate dataset. The last four represent the co-occurrence network pruned with various values of threshold  $\mathcal{T}$ . Note that vertices with the same color share the same ground truth community label.

For each similarity index listed in TABLE 2, we conduct similarity rewiring for certain times, and finally obtain a series of rewired networks.

### 3.3.2 Ensemble Optimization

After network rewiring, we feed all rewired networks into the **community detection** algorithm  $\mathcal{S}$  to generate a series of community partitions (line 4). Due to the diversity of similarity indices and rewiring schemes, these partitions are likely to be non-unique and not necessarily better than the original partition  $\mathcal{M}$ . Ensemble learning, which achieves better classification or prediction performance by integrating multiple weak models, has been used for clustering tasks. Previous works on consensus and ensemble clustering [28], [29] have shown that these techniques can be combined with existing clustering methods and improve the stability and accuracy of community partitions.

During **partition ensemble**, we aggregate multiple partitions using a consensus matrix  $\mathcal{A}_{co} = \{a_{ij}\}_{n \times n}$ , in which element  $a_{ij}$  indicates the frequency of two vertices  $v_i$  and  $v_j$  assigned to the same community. A weighted co-occurrence network  $\mathcal{G}_{co}$  can be generated by using  $\mathcal{A}_{co}$  as the adjacency matrix (line 5). Once pairwise vertices appear in the same community in some partitions,  $\mathcal{G}_{co}$  links them and assigns weights that correspond to the frequency of co-occurrence. A larger/smaller weight means a higher/lower likelihood that the pairwise vertices belong to the same community.

For the co-occurrence network  $\mathcal{G}_{co}$ , a natural idea is to consider those edges with larger/lower weights as

intra-/inter-community edges in the original network. Then, we can deploy community edge rewiring in  $\mathcal{G}_{co}$  to optimize network structure. For inter-community edge deletion, we can prune  $\mathcal{G}_{co}$  by setting a weight threshold  $\mathcal{T}$ . During **network pruning**, all edges with weights less than  $\mathcal{T}$  are considered as inter-community edges and will be removed from  $\mathcal{G}_{co}$  (line 6). We neglect intra-community edge addition since that the addition of new edges in  $\mathcal{G}_{co}$  depends on the co-occurrence of pairwise vertices, but there is no access to more new partitions at this stage.

A visualization of network pruning in the co-occurrence network of Karate dataset is shown in Fig. 4. In this paper, we use eight similarity indices, and for each index, ten samplings are performed, to generate a total of eighty partitions, which determine the range of threshold  $\mathcal{T} \in [0, 80]$ . The original Karate network is shown in Fig. 4 (a), and there are two communities, with the vertices of the same color sharing the same ground-truth community label. Fig. 4 (b) shows the co-occurrence network, which aggregates the information of eighty partitions and has dense connections. The last three subgraphs show the different pruned co-occurrence networks with various thresholds. When  $\mathcal{T} = 20$ , the pruned co-occurrence network still has only one connected component but two bridge vertices emerge, as shown in Fig. 4 (c). With the increase of the threshold,  $\mathcal{G}_{co}$  is pruned to two connected components, matching exactly with the two clusters in the original network, as shown in Fig. 4 (d). When the threshold approaches the upper limit, generally,

we'll get several small connected components that contain few vertices, or even isolated vertices, as shown in Fig. 4 (e). This phenomenon indicates that the selection of threshold actually influences the result of community partition, which is similar to the resolution limit problem in community detection. After pruning, the co-occurrence network  $\mathcal{G}_{co}$  is divided into several connected components, and those with large sizes will be treated as core communities  $\mathcal{M}_{core}^T$  (line 6). Generally, there exists several small connected components that contain few vertices, or even isolated vertices, when pruning  $\mathcal{G}_{co}$  with a relatively large threshold. In order to get a final partition, these vertices in small connected components will be treated as isolated ones and assigned to the core community, to which it has the maximum average similarity (line 7). The ID of the core community that an isolated vertex  $v_i$  is assigned to, is defined as:

$$ID_{\mathcal{H}} = \arg \max_k \frac{1}{\phi_{core}^k} \sum_{j \in \mathcal{M}_{core}^k} \mathcal{H}(i, j), \quad (6)$$

where  $\mathcal{M}_{core}^k$  is the  $k$ -th core community and  $\phi_{core}^k$  is the number of vertices in  $\mathcal{M}_{core}^k$ . The final ID is determined by a *relative majority vote* of all similarity indices used in this paper:

$$ID = \text{relativeMajorityVote}\{ID_{\mathcal{H}} \mid \mathcal{H} = \text{CN}, \dots, \text{RWR}\}. \quad (7)$$

### 3.3.3 Threshold Selection

In order to address the resolution limit problem, we search the optimal threshold via a traversal procedure. Actually, the range of threshold  $\mathcal{T} \in [0, 80]$  can be narrowed down to  $\mathcal{T} \in \{a_{ij} \mid \forall a_{ij} \in \mathcal{A}_{co}\}$ , which reduce the access times during traversal. We prune  $\mathcal{G}_{co}$  with an accessed threshold  $\mathcal{T}$  to yield a pruned network  $\mathcal{G}_{co}^{\mathcal{T}}$ , and evaluate the cluster partition of  $\mathcal{G}_{co}^{\mathcal{T}}$  using *cluster consensus* metric, which can quantify the stability of clusters [47]. For a pruned co-occurrence network  $\mathcal{G}_{co}^{\mathcal{T}}$  with cluster partition  $\mathcal{M}^{\mathcal{T}} = \{\mathcal{M}_k \mid k = 1, \dots, \phi^{\mathcal{T}}\}$ , the consensus of cluster  $\mathcal{M}_k$  is defined as

$$c(\mathcal{M}_k) = \frac{1}{\phi_k (\phi_k - 1) / 2} \sum_{\substack{i, j \in \mathcal{M}_k \\ i < j}} a_{ij}, \quad (8)$$

where  $\phi_k$  is the number of vertices in  $\mathcal{M}_k$ . The optimal threshold corresponds to that yield the  $\mathcal{G}_{co}^{\mathcal{T}}$  with the maximum partition score, which is computed via a weighted sum of cluster consensus, as follows:

$$C(\mathcal{M}^{\mathcal{T}}) = \sum_{k=1}^{\phi^{\mathcal{T}}} \frac{\phi_k}{n} c(\mathcal{M}_k), \quad (9)$$

$$\mathcal{T} = \arg \max_{\mathcal{T}} C(\mathcal{M}^{\mathcal{T}}). \quad (10)$$

Note that Eq (10) is the heuristic definition of the optimal threshold, which can alleviate the resolution limit problem to a certain extent. Considering the complexity of the calculation during threshold selection, we can further simplify this process by the following approximation:

$$\mathcal{T}' = \arg \min_{\mathcal{T}} |\phi_{core}^{\mathcal{T}} - \phi_{real}|, \quad (11)$$

where  $\phi_{core}^{\mathcal{T}}$  is the number of core communities yielded during network pruning.  $\mathcal{T}'$  is the approximate optimal threshold, and we can obtain the core communities, of which the number is closest to that of the ground-truth. Note that this

approximation depends on the knowledge of the ground-truth community.

## 4 EXPERIMENTS

### 4.1 Datasets

We evaluate the proposed approaches against six real-world networks and four adversarial networks. For all networks, the ground-truth community labels are available. TABLE 3 provides an overview of the networks considered, including the number of communities found by each community detection method. Specifically, the six real-world networks consist of four small benchmark networks and two large-scale networks with missing data. The networks with missing data are sub-networks extracted from the Amazon product co-purchasing network and DBLP collaboration network [46], respectively. The four adversarial networks are generated via adversarial attack on four benchmark networks. Refer to Appendix A.2 for more details about datasets.

### 4.2 Evaluation Metrics

Benefiting from the availability of the ground-truth community labels, we evaluate the community partitions using supervised metrics like normalized mutual information [10] and adjusted rand index. Note that we design the fitness in *RobustECD-GA* using modularity  $\mathcal{Q}$ , thus it is not suitable as the evaluation metric.

- **Modularity ( $\mathcal{Q}$ )** [9]. Modularity is commonly used to measure the quality of community partition for a network with unknown community structure. The basic idea is to compare the network with the corresponding *null models*, which refer to random graph models that have some of the same properties as the network but are completely random in other aspects. For a given network and a specific community partition  $\mathcal{M}$ , modularity is defined as:

$$\mathcal{Q} = \frac{1}{2m} \sum_{ij} \left( \mathcal{A}_{ij} - \frac{k_i k_j}{2m} \right) \delta(l_i, l_j), \quad (12)$$

where  $m$  is the number of edges,  $\mathcal{A}_{ij}$  is the element of adjacency matrix  $\mathcal{A}$ ,  $k_i, k_j$  are the degree of vertices  $v_i, v_j$ , respectively.  $l_i, l_j$  are the community labels of vertices  $v_i, v_j$  in  $\mathcal{M}$ , respectively.  $\delta(l_i, l_j) = 1$  if  $l_i = l_j$  and  $\delta(l_i, l_j) = 0$  otherwise.

- **Normalized Mutual Information (NMI)** [10]. NMI is a commonly used criterion to evaluate the similarity of two clustering results. It quantifies how much information the estimated partition contains in the real partition. For two clustering results  $X$  and  $Y$ , the NMI is defined as:

$$I_{\text{norm}}(X, Y) = \frac{2I(X, Y)}{H(X) + H(Y)}, \quad (13)$$

where  $I(X, Y) = H(Y) - H(X|Y)$  is the mutual information of  $X$  and  $Y$ ,  $H(Y)$  is the Shannon entropy of  $Y$ , and  $H(X|Y)$  is the conditional entropy of  $X$  given  $Y$ .

- **Adjusted Rand Index (ARI)** [48]. ARI is the corrected-for-chance version of the Rand index (RI), which mea-

TABLE 3  
Real-world networks.  $\phi_S$  is the number of communities found by the specific community detection method  $S$ .

Network	$m$	$n$	$\phi_{real}$	Description	Number of communities ( $\phi_S$ )					
					INF	FG	WT	LOU	LP	N2VKM
Karate	34	78	2	Zachary Karate club [43]	3	3	4	4	2	2
Polbooks	105	441	3	Books about US politics [44]	6	4	5	4	4	3
Football	115	613	12	American College football [13]	12	6	10	10	9	12
Polblogs	1490	19090	2	Political blogs [45]	306	277	416	276	272	2
Amazon-sub	10077	24205	3251	Amazon product co-purchasing [46]	651	97	509	69	638	—
DBLP-sub	26183	137529	5051	DBLP collaboration [46]	1143	120	4361	49	787	—

sures the degree of agreement between an estimated partition and a real partition. It is defined as

$$ARI = \frac{RI - E[RI]}{\max(RI) - E[RI]}. \quad (14)$$

Both NMI and ARI require the ground-truth community labels for evaluation purpose and the values are generally in the range between 0 to 1. For both metrics, a larger value indicates a better partition.

### 4.3 Community Detection Methods

We consider the following six community detection algorithms in our experiments.

- **Infomap (INF)** [17]. Infomap decomposes a network into modules by compressing the description of the information flow, i.e., it detects communities by minimizing the encoding length for a random walk.
- **Fast Greedy (FG)** [14]. This is a bottom-up hierarchical agglomeration algorithm. It merges individual vertices into communities based on a greedy modularity maximization strategy.
- **WalkTrap (WT)** [49]. It detects communities based on the idea that short random walks tend to stay in the same community.
- **Louvain (LOU)** [12]. This is a multi-level modularity optimization algorithm. It initializes each vertex with a separate community, and moves vertices between communities iteratively in a way that maximizes the vertices' local contributions to the overall modularity.
- **Label Propagation (LP)** [19]. This method detects communities by initializing each vertex with a unique label and re-assigning each vertex the dominant label in its neighbourhood in each iteration.
- **Node2vec + Kmeans (N2VKM)** [50]. This is a network embedding method, which learns lower-dimensional representations for vertices by biased random walk and skip-Gram. The  $K$ -means algorithm is then used to detect communities by clustering the embedded vectors of vertices in an Euclidean space.

### 4.4 Baseline Enhancement Methods

We compare our methods with the following two typical traditional enhancement methods, one is based on network rewiring and the other utilizes network weighting.

- **EdMot** [27]. It is an edge enhancement approach for motif-aware community detection via network rewiring and is proposed to address the hypergraph

TABLE 4  
Main parameters setting for the proposed algorithms.

Method	Parameter	Value
RobustECD-GA	$GA(\phi_p, \mathcal{P}_c, \mathcal{P}_m, \mathcal{P}_e, \mathcal{T}_{ga})$	{120, 0.8, 0.02, 0.2, 1000}
	$\beta_a$	{0.01, 0.02, ..., 2.9}
	$\beta_d$	{0.01, 0.02, ..., 0.29}
RobustECD-SE	$\beta_a$	{0.1, 0.2, ..., 2.9}

fragmentation issue. This strategy is recently proposed and achieves the state-of-the-art enhancement effect in several community detection methods.

- **WERW-KPath** [24]. It is an enhancement approach for community detection via network weighting. It exploits random walks to compute the  $\kappa$ -path edge centrality, which is then used to weight the edges. The strategy shows better interpretability and effectiveness among a series of weighted methods.

### 4.5 Experiment Setup

For all datasets, edges in networks are treated as undirected and self-loops will be removed. The main parameter settings for the proposed algorithms are shown in TABLE 4.

In *RobustECD-GA*, the general parameters of GA are set as empirical values. Note that the budget  $\beta_a$  and  $\beta_d$  controls the upper limit of the chromosome size during Initialization, i.e., each chromosome will be initialized with an unfixed size not larger than  $\lceil m \cdot (\beta_a + \beta_d) \rceil$ . We vary  $\beta_a$  and  $\beta_d$  in {0.01, 0.02, ..., 2.9} and {0.01, 0.02, ..., 0.29}, respectively. In *RobustECD-SE*, we vary  $\beta_a$  in {0.1, 0.2, ..., 2.9}.

In addition, for the community detection algorithm N2VKM, we take the number of clusters  $K$  in  $K$ -means the same as that of the ground-truth communities, and use the default setting for parameters in *Node2vec*. Specifically, the walk length is 80, the number of walks per node is 10, the embedding dimension is 128, and both return hyper parameter  $p$  and in-out parameter  $q$  are equal to 1. We repeat all experiments for 50 times and report the average metrics and their standard deviations of community detection.

### 4.6 Evaluation

We evaluate the benefit of the proposed enhancement strategies, answering the following research questions:

- **RQ1:** Can *RobustECD* improve the performance of community detection in real-world networks combined with existing community detection algorithms?
- **RQ2:** Does *RobustECD* still work when it comes to adversarial networks?
- **RQ3:** How does the selection of various similarity indices in *RobustECD-SE* affect the performance?



TABLE 5  
Community detection results in the real networks.

Dataset	Method	Community Detection													
		NMI						Avg RIMP	ARI						
		INF	FG	WT	LOU	LP	N2VKM		INF	FG	WT	LOU	LP	N2VKM	Avg RIMP
Karate	original	0.699±0.000	0.598±0.000	0.600±0.000	0.587±0.000	0.689±0.283	0.705±0.175	—	0.702±0.000	0.491±0.000	0.513±0.000	0.462±0.000	0.687±0.320	0.716±0.212	—
	WERW-Kpath	0.618±0.071	0.607±0.040	0.528±0.059	0.518±0.043	0.622±0.185	0.644±0.186	-8.70%	0.557±0.124	0.593±0.046	0.398±0.107	0.407±0.042	0.604±0.229	0.652±0.227	-9.20%
	Edmot	0.699±0.000	0.598±0.000	0.600±0.000	0.587±0.000	0.685±0.203	0.713±0.177	0.09%	0.702±0.000	0.491±0.000	0.513±0.000	0.462±0.000	0.686±0.237	0.728±0.200	0.26%
	RobustECD-GA	<b>0.912±0.176</b>	0.878±0.071	<b>0.984±0.049</b>	0.867±0.090	0.705±0.180	<b>0.838±0.019</b>	35.03%	<b>0.923±0.165</b>	0.912±0.051	<b>0.988±0.035</b>	0.898±0.083	0.714±0.217	<b>0.872±0.024</b>	54.98%
	RobustECD-SE	0.825±0.220	<b>1.000±0.000</b>	0.821±0.088	<b>1.000±0.000</b>	<b>0.847±0.136</b>	0.834±0.114	<b>38.95%</b>	0.797±0.240	<b>1.000±0.000</b>	0.852±0.086	<b>1.000±0.000</b>	<b>0.871±0.124</b>	0.869±0.100	<b>57.98%</b>
Polbooks	original	0.493±0.000	0.531±0.000	0.559±0.000	0.512±0.000	0.554±0.025	0.556±0.017	—	0.536±0.000	0.638±0.000	0.681±0.000	0.558±0.000	0.647±0.041	0.662±0.009	—
	WERW-Kpath	0.462±0.002	0.546±0.020	0.531±0.031	0.509±0.020	0.552±0.034	0.563±0.016	-1.36%	0.435±0.000	0.658±0.026	0.591±0.069	0.571±0.034	0.654±0.054	0.660±0.015	-4.30%
	Edmot	0.493±0.000	0.531±0.000	0.559±0.000	0.512±0.000	0.561±0.026	0.564±0.016	0.45%	0.536±0.000	0.638±0.000	0.681±0.000	0.558±0.000	0.661±0.035	0.667±0.018	0.49%
	RobustECD-GA	0.526±0.121	0.554±0.000	0.554±0.000	0.554±0.000	0.554±0.014	0.589±0.017	4.04%	0.621±0.143	<b>0.652±0.000</b>	0.652±0.000	0.652±0.000	<b>0.670±0.007</b>	<b>0.684±0.013</b>	6.25%
	RobustECD-SE	<b>0.574±0.014</b>	<b>0.569±0.001</b>	<b>0.586±0.017</b>	<b>0.560±0.011</b>	<b>0.598±0.009</b>	<b>0.589±0.009</b>	<b>8.61%</b>	<b>0.677±0.014</b>	0.636±0.000	<b>0.687±0.015</b>	<b>0.659±0.006</b>	0.665±0.010	0.677±0.011	<b>8.64%</b>
Football	original	0.924±0.000	0.698±0.000	0.887±0.000	0.890±0.000	0.888±0.037	0.912±0.012	—	0.897±0.000	0.474±0.000	0.815±0.000	0.807±0.000	0.784±0.103	0.872±0.025	—
	WERW-Kpath	0.924±0.000	0.698±0.000	0.887±0.000	0.890±0.000	0.885±0.030	0.915±0.011	0.00%	0.897±0.000	0.474±0.000	0.815±0.000	0.807±0.000	0.779±0.083	0.876±0.020	-0.03%
	Edmot	0.924±0.000	0.698±0.000	0.887±0.000	0.890±0.000	0.885±0.030	0.915±0.011	0.00%	0.897±0.000	0.474±0.000	0.815±0.000	0.807±0.000	0.779±0.083	0.876±0.020	-0.03%
	RobustECD-GA	<b>0.927±0.000</b>	0.862±0.018	<b>0.927±0.000</b>	<b>0.909±0.000</b>	0.896±0.023	<b>0.927±0.000</b>	<b>5.50%</b>	0.889±0.000	0.746±0.042	<b>0.889±0.000</b>	0.847±0.000	0.793±0.082	<b>0.889±0.000</b>	12.27%
	RobustECD-SE	0.924±0.000	<b>0.877±0.021</b>	0.923±0.009	0.906±0.014	<b>0.915±0.018</b>	0.898±0.021	<b>5.50%</b>	<b>0.897±0.000</b>	<b>0.785±0.061</b>	0.881±0.018	<b>0.849±0.029</b>	<b>0.869±0.032</b>	<b>0.849±0.029</b>	<b>14.52%</b>
Polblogs	original	0.330±0.001	0.378±0.000	0.318±0.000	0.376±0.000	0.375±0.053	0.458±0.067	—	0.439±0.001	0.528±0.000	0.419±0.000	0.521±0.000	0.515±0.105	0.489±0.053	—
	WERW-Kpath	0.329±0.001	0.376±0.002	0.316±0.001	0.370±0.001	0.375±0.037	0.453±0.025	-0.69%	0.437±0.003	0.525±0.003	0.414±0.003	0.515±0.002	0.518±0.074	0.480±0.040	-0.77%
	Edmot	0.329±0.000	0.378±0.000	0.318±0.000	0.376±0.000	0.376±0.053	0.457±0.031	-0.04%	0.437±0.000	0.528±0.000	0.419±0.000	0.521±0.000	0.517±0.105	0.486±0.049	-0.11%
	RobustECD-GA	0.453±0.000	0.525±0.000	0.504±0.000	0.529±0.000	0.519±0.005	0.381±0.002	32.82%	0.472±0.000	0.618±0.000	0.599±0.000	0.622±0.000	0.616±0.002	0.556±0.001	20.04%
	RobustECD-SE	<b>0.517±0.007</b>	<b>0.551±0.006</b>	<b>0.556±0.009</b>	<b>0.551±0.005</b>	<b>0.529±0.007</b>	<b>0.499±0.006</b>	<b>45.64%</b>	<b>0.619±0.005</b>	<b>0.642±0.004</b>	<b>0.643±0.006</b>	<b>0.644±0.004</b>	<b>0.628±0.005</b>	<b>0.569±0.005</b>	<b>29.66%</b>
Amazon -sub	original	0.775±0.000	0.592±0.000	0.703±0.000	0.607±0.000	0.760±0.001	—	—	0.110±0.000	0.034±0.000	0.048±0.000	0.045±0.000	0.069±0.004	—	—
	WERW-Kpath	0.777±0.000	0.632±0.000	<b>0.748±0.000</b>	0.633±0.000	<b>0.770±0.000</b>	—	3.80%	<b>0.112±0.000</b>	0.048±0.000	0.052±0.000	0.052±0.000	<b>0.076±0.000</b>	—	15.91%
	Edmot	0.775±0.000	0.593±0.000	0.703±0.000	0.607±0.000	0.761±0.000	—	0.06%	0.110±0.000	0.034±0.000	0.048±0.000	0.045±0.000	0.073±0.000	—	1.28%
	RobustECD-SE	<b>0.779±0.000</b>	<b>0.663±0.009</b>	0.732±0.005	<b>0.657±0.004</b>	0.768±0.001	—	<b>5.18%</b>	0.107±0.000	<b>0.053±0.004</b>	<b>0.058±0.008</b>	<b>0.053±0.000</b>	0.067±0.001	—	<b>18.72%</b>
DBLP -sub	original	0.698±0.000	0.348±0.000	0.683±0.000	0.431±0.000	0.436±0.000	—	—	0.061±0.000	0.004±0.000	0.004±0.000	0.010±0.000	0.000±0.000	—	—
	WERW-Kpath	0.701±0.000	0.350±0.000	<b>0.688±0.000</b>	0.438±0.000	<b>0.649±0.000</b>	—	10.44%	0.062±0.000	0.004±0.000	0.005±0.000	0.011±0.000	<b>0.008±0.000</b>	—	6.43%
	Edmot	0.699±0.000	0.354±0.000	0.683±0.000	0.431±0.000	0.446±0.000	—	0.83%	0.060±0.000	0.003±0.000	0.004±0.000	0.010±0.000	0.000±0.000	—	-2.60%
	RobustECD-SE	<b>0.704±0.000</b>	<b>0.582±0.000</b>	0.684±0.000	<b>0.598±0.000</b>	0.638±0.000	—	<b>30.66%</b>	<b>0.064±0.000</b>	<b>0.007±0.000</b>	<b>0.011±0.000</b>	<b>0.019±0.000</b>	0.003±0.000	—	<b>72.08%</b>

TABLE 6  
Community detection results in the adversarial networks.

Dataset	Method	Community Detection													
		NMI						Avg RIMP	ARI						
		INF	FG	WT	LOU	LP	N2VKM		INF	FG	WT	LOU	LP	N2VKM	Avg RIMP
Karate (noise)	original	0.699±0.000	0.598±0.000	0.600±0.000	0.587±0.000	0.689±0.283	0.705±0.175	63.90%	0.702±0.000	0.491±0.000	0.513±0.000	0.462±0.000	0.687±0.320	0.716±0.212	70.66%
	Attack	0.000±0.000	0.447±0.000	0.487±0.000	0.250±0.000	0.475±0.337	0.399±0.231	—	0.000±0.000	0.361±0.000	0.330±0.000	0.180±0.000	0.498±0.354	0.427±0.261	—
	WERW-Kpath	0.173±0.093	0.296±0.050	0.444±0.082	0.341±0.060	0.373±0.211	0.384±0.198	-2.36%	0.116±0.114	0.258±0.044	0.359±0.133	0.281±0.043	0.357±0.255	0.401±0.238	2.26%
	Edmot	0.001±0.000	0.447±0.000	0.479±0.000	0.250±0.000	0.418±0.345	0.427±0.225	-1.09%	0.000±0.000	0.361±0.000	0.525±0.000	0.180±0.000	0.446±0.367	0.448±0.257	8.93%
	RobustECD-GA	<b>0.720±0.132</b>	0.576±0.000	<b>0.670±0.019</b>	0.352±0.128	0.371±0.327	<b>0.836±0.183</b>	44.48%	<b>0.768±0.122</b>	0.668±0.000	<b>0.743±0.096</b>	0.367±0.131	0.393±0.350	<b>0.882±0.152</b>	<b>79.39%</b>
RobustECD-SE	0.425±0.336	<b>0.709±0.218</b>	0.576±0.075	<b>0.484±0.173</b>	<b>0.828±0.197</b>	0.529±0.340	<b>53.31%</b>	0.427±0.373	<b>0.720±0.252</b>	0.593±0.102	<b>0.448±0.208</b>	<b>0.857±0.198</b>	0.552±0.352	78.68%	
Polbooks (noise)	original	0.493±0.000	0.531±0.000	0.559±0.000	0.512±0.000	0.554±0.025	0.556±0.017	26.69%	0.536±0.000	0.638±0.000	0.681±0.000	0.558±0.000	0.647±0.041	0.662±0.009	47.95%
	Attack	0.418±0.004	0.482±0.000	0.393±0.000	0.343±0.000	0.461±0.030	0.462±0.012	—	0.459±0.010	0.530±0.000	0.351±0.000	0.252±0.000	0.534±0.053	0.581±0.011	—
	WERW-Kpath	0.485±0.006	0.560±0.019	0.503±0.013	0.481±0.010	0.552±0.032	0.565±0.020	23.74%	0.505±0.013	0.641±0.028	0.541±0.041	0.552±0.015	0.649±0.054	0.660±0.015	39.88%
	Edmot	0.490±0.000	0.482±0.000	0.494±0.000	0.367±0.000	0.566±0.031	0.571±0.018	16.05%	0.533±0.000	0.530±0.000	0.539±0.000	0.344±0.000	0.653±0.051	0.666±0.013	23.85%
	RobustECD-GA	0.559±0.000	0.559±0.000	0.559±0.000	0.559±0.000	0.585±0.017	0.592±0.022	34.99%	0.646±0.000	<b>0.646±0.000</b>	0.646±0.000	0.646±0.000	<b>0.692±0.011</b>	0.658±0.015	57.64%
RobustECD-SE	<b>0.590±0.014</b>	<b>0.565±0.012</b>	<b>0.599±0.008</b>	<b>0.564±0.010</b>	<b>0.599±0.008</b>	<b>0.643±0.026</b>	<b>40.72%</b>	<b>0.656±0.015</b>	0.628±0.013	<b>0.691±0.012</b>	<b>0.672±0.007</b>	0.665±0.009	<b>0.729±0.018</b>	<b>62.49%</b>	
Football (noise)	original	0.924±0.000	0.698±0.000	0.887±0.000	0.890±0.000	0.888±0.037	0.912±0.012	11.27%	0.897±0.000	0.474±0.000	0.815±0.000	0.807±0.000	0.784±0.103	0.872±0.025	52.52%
	Attack	0.809±0.000	0.658±0.000	0.809±0.000	0.755±0.000	0.800±0.051	0.838±0.027	—	0.498±0.000	0.375±0.000	0.498±0.000	0.481±0.000	0.503±0.142	0.719±0.055	—
	WERW-Kpath	0.795±0.003	0.643±0.017	0.878±0.022	0.812±0.025	0.765±0.059	0.841±0.026	1.34%	0.486±0.001	0.378±0.028	0.770±0.066	0.623±0.055	0.449±0.143	0.725±0.057	12.10%
	Edmot	0.809±0.000	0.658±0.000	0.809±0.000	0.755±0.000	0.781±0.051	0.835±0.027	-0.46%	0.498±0.000	0.375±0.000	0.498±0.000	0.481±0.000	0.444±0.116	0.714±0.061	-2.07%
	RobustECD-GA	<b>0.927±0.000</b>	<b>0.791±0.000</b>	<b>0.927±0.000</b>	<b>0.909±0.000</b>	0.797±0.071	<b>0.870±0.015</b>	<b>12.20%</b>	<b>0.889±0.000</b>	<b>0.597±0.000</b>	<b>0.889±0.000</b>	<b>0.847±0.000</b>	0.430±0.211	0.753±0.049	<b>47.09%</b>
RobustECD-SE	0.809±0.000	0.762±0.024	0.909±0.020	0.886±0.014	<b>0.863±0.051</b>	0.862±0.021	9.38%	0.498±0.000	0.488±0.056	0.843±0.063	0.793±0.033	<b>0.680±0.189</b>	<b>0.769±0.043</b>	34.40%	
Polblogs (noise)	original	0.330±0.001	0.378±0.000	0.318±0.000	0.376±0.000	0.375±0.053	0.458±0.067	8.60%	0.439±0.001	0.528±0.000	0.419±0.000	0.521±0.000	0.515±0.105	0.489±0.053	9.42%

- **RQ4:** How does *RobustECD* achieve interpretable enhancement of community detection?

#### 4.6.1 Enhancement in Real Network

TABLE 5 reports the results of the enhancement for six community detection algorithms, from which one can observe that there is a significant boost in detection performance across all six real-world networks. Firstly, compared with those traditional enhancement algorithms, these detection algorithms combined with the proposed *RobustECD* framework obtain much better results in most cases. The *RobustECD-GA* and *RobustECD-SE* achieves 87.50% and 88.24% success rate on enhancing community detection. The success rate refers to the percentage of enhanced results which are better than the original results in term of both NMI and ARI. These phenomenon provide a positive answer to **RQ1**, indicating that *RobustECD* can improve the performance of existing community detection algorithms and alleviate the problems of resolution limit and missing data. Meanwhile, the results in Amazon and DBLP sub-networks also indicates the effectiveness of the *RobustECD-SE* in large-scale networks.

Secondly, we define the relative improvement rate (RIMP) for each metric as follows:

$$RIMP = \begin{cases} (Met_{en} - Met_{ori})/Met_{ori} & Met_{ori} > 0 \\ Met_{en} - Met_{ori} & Met_{ori} = 0 \end{cases} \quad (15)$$

where  $Met_{ori}$  and  $Met_{en}$  refer to the metric of the original and the enhanced results, respectively. Note that we also consider the extreme case that the original metrics may go down to 0 in the adversarial networks. In TABLE 5, the far-right column of each metrics gives the average relative improvement rate (Avg RIMP) in metric, from which one can see that *RobustECD-GA* and *RobustECD-SE* achieve competitive performance, and significantly outperform baselines.

Thirdly, considered detection algorithms have different performance on the real datasets, but generally obtain more similar community partitions during robust enhancement. For instance, we use standard deviation to measure the consistency of results of different detection algorithms. For *RobustECD-SE*, the standard deviations of the original ARI for the six detection algorithms on the six networks are (0.118, 0.059, 0.153, 0.046, 0.030, 0.026), while those of the corresponding enhanced ARI are (0.067, 0.018, 0.039, 0.029, 0.023, 0.025). The decrease in standard deviation indicates that *RobustECD* can stable network structure and achieve the consistency of detection performance. Moreover, *RobustECD* achieves perfect enhancement on some community detection algorithms applied to small datasets. For instance, when enhancing FG and LOU via *RobustECD-SE* on Karate dataset, both NMI and ARI are equal to 1, suggesting that FG and LOU algorithms can detect community structures completely correctly after enhancement.

#### 4.6.2 Enhancement in Adversarial Network

Adversarial attack aims to degrade the performance of algorithms by perturbing the network structure or attacking the computational process. In social networks, the adversarial attack on community detection or link prediction probably facilitates to hide the real community structure or sensitive links. TABLE 6 reports the results of enhancing

community detection in adversarial networks, which are generated by slightly modifying the networks structures via certain adversarial attacks. Note that here we report the community detection results in original networks and adversarial networks as references. As we can see, compared with the original results, the performance metrics display a significant decrease in adversarial networks, indicating that adversarial attack has indeed broken the network structure and achieved a community detection deception. Then during structure enhancement, our algorithms significantly outperform the baselines in all adversarial networks. In fact, both *RobustECD-GA* and *RobustECD-SE* help the six community detection algorithms achieve huge improvements on detection performances, which is even better than the results in original networks. However, the baselines Edmot and WERW-KPath have mediocre performance and may fail with the increase of the attack strength. Such results indicate that our enhancement algorithms could not only help partially or even fully recover the network structures destroyed by adversarial attacks, but also improving the robustness of existing community detection algorithms against adversarial noise, positively answering **RQ2**.

#### 4.6.3 Impact of Similarity in RobustECD-SE

Thanks to the outstanding performance of *RobustECD*, we further investigate the impact of the similarity indices in the *RobustECD-SE*. Fig. 5 shows the results of all similarity indices (*RobustECD-SE(all)*) and single index (*RobustECD-SE(single)*), respectively (see the Appendix A.5 and Appendix A.6 for more details about the impact of similarity indices). We first summarized three impact effects:

- **Complementary:** *RobustECD-SE(all)* outperforms all *RobustECD-SE(single)s*, indicating that these single similarity indices are complementary.
- **Redundant:** *RobustECD-SE(single)s* with some indices achieve competitive performance against *RobustECD-SE(all)*, indicating that the other indices in *RobustECD-SE(single)s* that have relative poor performance are redundant.
- **Negative:** *RobustECD-SE(single)s* with some indices outperform *RobustECD-SE(all)*, indicating that the other indices in *RobustECD-SE(single)s* that have relative poor performance are negative.

From the comparison results, we observe that *RobustECD-SE(all)* generally outperforms *RobustECD-SE(single)*, and receives more stable results in most cases. And the impact of single similarity index behaves differently on various networks and various budgets, answering **RQ3**. In Karate ( $\beta_a \in (1.0, 2.0)$ ), *RobustECD-SE(single)s* with first-order similarity have relatively good performance while those with second-order and high-order similarity have relatively poor performance. Since that the scale of Karate is particularly small and first-order similarity are sufficient to capture structure features. In this case, first-order similarity indices are complementary, second-order and high-order similarity could be redundant or even negative. In Polblogs ( $\beta_a \in (0.5, 2.5)$ ), *RobustECD-SE(single)s* achieve competitive performance against *RobustECD-SE(all)* except for those with Jaccard, Salton and high-order similarity, which turn out to be redundant.

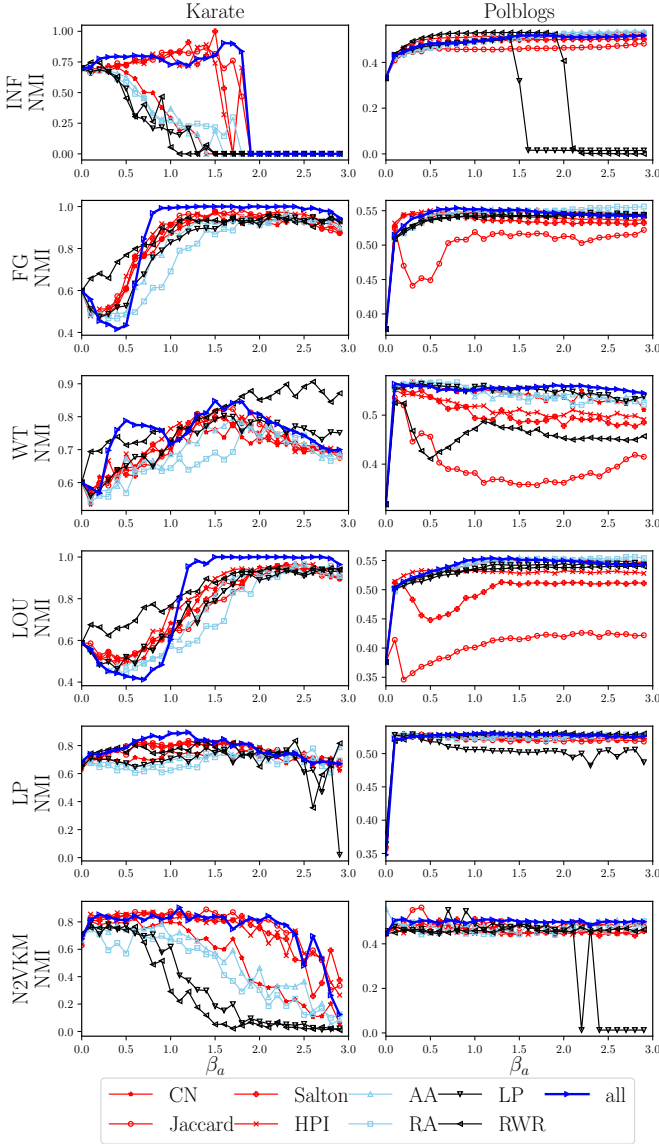


Fig. 5. The impact of similarity metrics on the performance of *RobustECD-SE* in term of NMI.

#### 4.6.4 Explanatory Visualization of *RobustECD-GA*

Next, we further investigate how the *RobustECD* optimizes the performances of different detection algorithms. Since the mechanism of *RobustECD-SE* has been presented in Fig 4, we only visualize the *RobustECD-GA* for algorithm LOU in Karate network, as shown in Fig. 6.

The community structure found by LOU in the original network is shown in Fig. 6 (a), where there are four communities. Since the number of communities found by LOU is more than the ground truth ( $\phi_{real} = 2$ ), as mentioned in TABLE 3, extra inter-community edge addition is available when  $\phi_S > \phi_{real}$  ( $S = \text{LOU}$ ). The result of *RobustECD-GA* in the original network is shown in Fig. 6 (b), where the enhancement scheme consists of 1 intra-community edge addition and 13 inter-community edge additions, and achieves a significant improvement on community detection, leading to the increase of 35.56% and 91.02% in NMI and ARI, respectively. Essentially, a large number of inter-community edge additions successfully merge small clusters into larger ones, resulting in more accurate partitions.

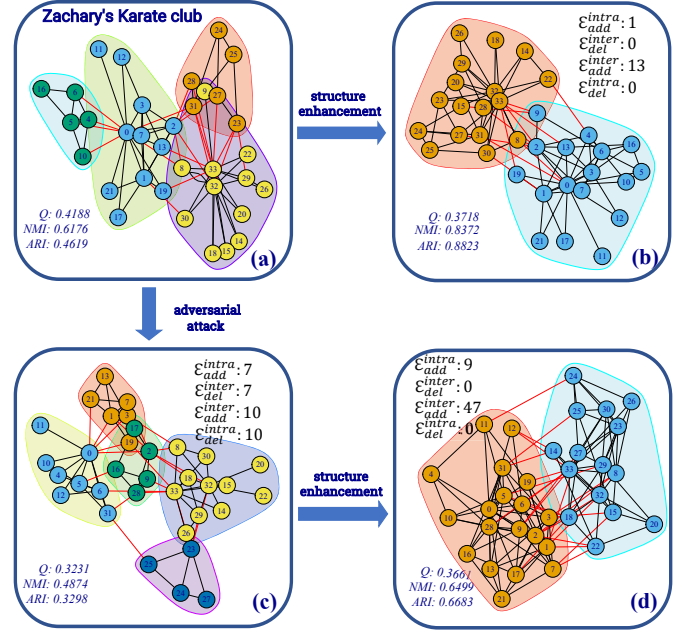


Fig. 6. Enhancement for LOU in Karate network.

Notably, the decrease of modularity here (from 0.4188 to 0.3718) can explain why we don't design modularity as fitness function directly. By comparing the information in Figs. 6 (a) and (b), a community partition with larger modularity does not mean closer to the ground-truth community structure. Therefore, if we have knowledge of community information, we can combine modularity with the true number of clusters, to obtain more accurate optimization guidance. This has been shown to have excellent performance in enhancing community detection. However, when facing unlabeled networks, the fitness function degrades to modularity, i.e.,  $f = Q$ , so the *RobustECD-GA* may be weakened to a certain extent.

Now, consider the adversarial network obtained by  $Q$ -Attack, as shown in Fig. 6 (c).  $Q$ -Attack keeps the number of edges unchanged during community deception and achieves a 22.85% reduction in modularity with an attack budget of 17. As we can see, community structure suffers from structural damage and a new cluster that contains the fringe vertices in the original network is discovered. We then deploy structure enhancement to this adversarial network and obtain the enhanced network shown in Fig. 6 (d). Compared with the community partition in Fig. 6 (c), LOU achieves a better partition, which even surpasses that in the original network shown in Fig. 6 (a). Such result suggests that our enhancement algorithms can indeed help the existing community detection algorithms defend against adversarial attacks. More interestingly, it seems that such structure enhancement not only repairs the broken network structure caused by adversarial attack, but also further optimizes it to obtain a clearer community structure, answering **RQ4**.

#### 4.6.5 Parameter Sensitivity

In this subsection, we discuss the impact of key parameters on the performance of *RobustECD-SE* (see the Appendix A.3 for the sensitivity analysis in *RobustECD-GA*). The metrics with a budget of 0 corresponds to the original results.

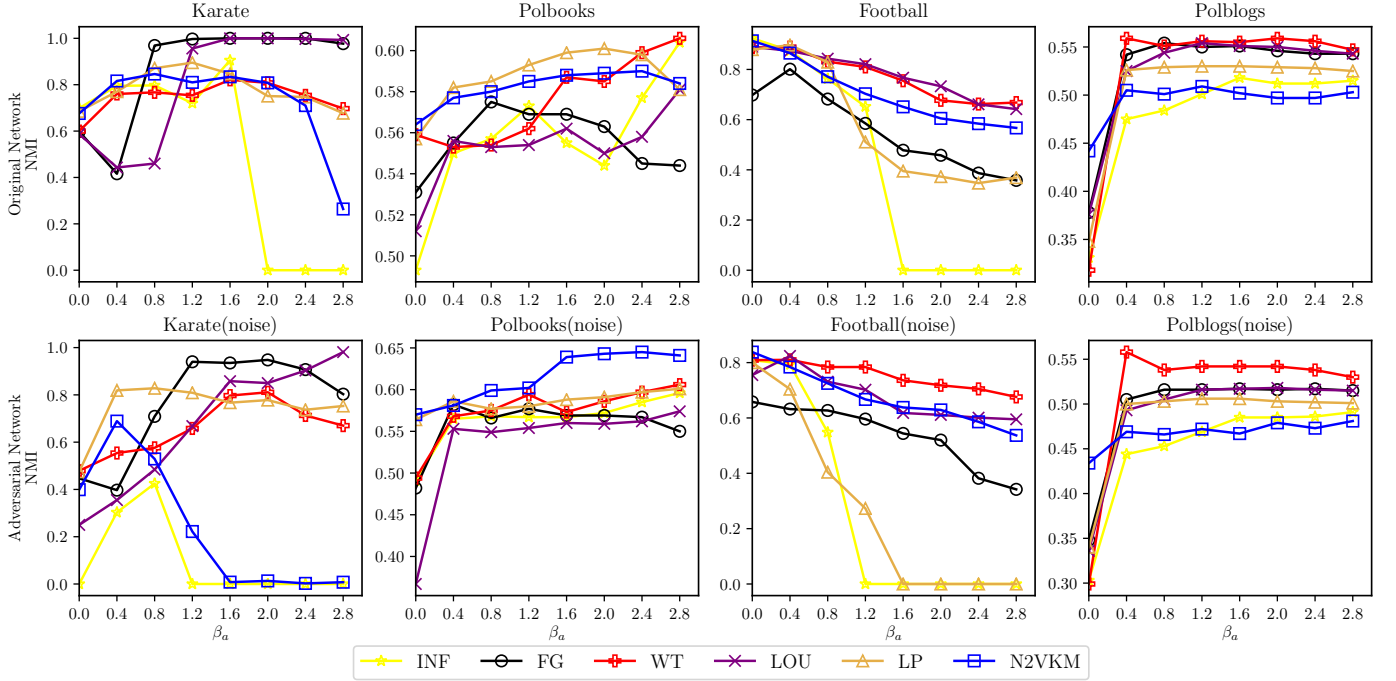


Fig. 7. The impact of modification budget  $\beta_a$  on the performance of *RobustECD-SE*.

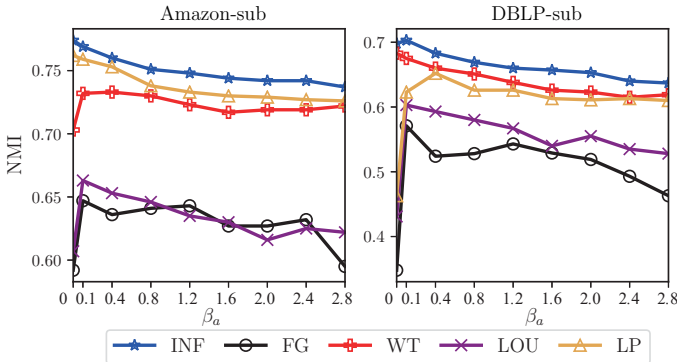


Fig. 8. The impact of modification budgets  $\beta_a$  on the performance of *RobustECD-SE* for large-scale networks.

Firstly, we present the evaluate results of *RobustECD-SE* in Fig. 7, from which one can see that such impact behaves differently on various networks. Specifically, Polblogs has a low average NMI equal to 0.373, and the performance of *RobustECD-SE* is relatively stable with the increase of budget; Polbooks has an average NMI equal to 0.534, and its performance curve is messy but basically goes up; for Karate with the average NMI equal to 0.646, when the budget is relatively large, FG and LOU performs well while INF and N2VKM suffers from negative enhancement; Football has an average NMI up to 0.869, the performance of *RobustECD-SE* drops steadily with the increase of budget. Essentially, the impact of modification budget on the performance of *RobustECD-SE* is influenced by the network structure. That is, for networks with weak community structures and low average performance metrics, like Polblogs, most community detection algorithms have huge spaces to be enhanced. But, for those networks with strong community structures like Football, it is difficult for *RobustECD-SE* to further enhance the community detection, i.e., adding or deleting more links may even weaken the stable community structure, leading to the degradation of performance.

Finally, Fig. 8 shows the evaluate results of *RobustECD-*

TABLE 7  
The average running time (s) of the four enhancement algorithms. The test is performed on LOU with the same experimental setup.

Time (s) \ Dataset	Karate	Polbooks	Football	Polblogs	Amazon	DBLP
Edmot	0.01	0.03	0.05	1.37	2.50	24.10
WERW-Kpath	2.10	11.40	25.77	1200.00	5000.00	68900.00
<i>RobustECD-GA</i>	47.40	136.00	170.00	13900.00	—	—
<i>RobustECD-SE</i>	0.12	0.24	0.38	17.10	357.00	5440.00

*SE* in large-scale networks. As we can see, *RobustECD-SE* still works in large-scale networks in most cases, and the performance drops slowly as the budget increase.

#### 4.6.6 Computational Complexity Analysis

In order to compare the efficiency of our *RobustECD*, we roughly estimated their time complexity as follows.

- The most computationally expensive part of *RobustECD-GA* is the calculation of fitness, which consists of modularity  $Q$  and the number of communities  $\phi_s$ , so an extra community detection is necessary before the calculation of fitness. Besides, selection, crossover and mutation are consisted of sampling and edge operations, and have a cost of  $\mathcal{O}(|\mathcal{E}|)$ , where  $|\mathcal{E}|$  is the number of edges in the original network. So *RobustECD-GA* runs in time  $\mathcal{O}(\phi_p \cdot \mathcal{T}_{ga} \cdot \max(|S|, |\mathcal{E}|))$ , where  $|S|$  is the time complexity of the target community detection algorithm.
- The most computationally expensive part of *RobustECD-SE* is the threshold selection, which has a cost of  $\mathcal{O}(|\mathcal{E}_{co}|)$ , where  $|\mathcal{E}_{co}|$  is the number of edges in the co-occurrence network.  $\mathcal{G}_{co}$  can be much denser than the original network and have up to  $n(n-1)/2$  edges. So the time complexity of *RobustECD-SE* is no more than  $\mathcal{O}(n^2)$ .

Moreover, we evaluate the efficiency of *RobustECD* by directly comparing the running time with baselines. The

average running time (in seconds) of the four algorithms are presented in TABLE 7. As we can see, although the *RobustECD-GA* performs well on small-scale networks, it is limited by the optimization mode and does not scale well on large networks. Instead, *RobustECD-SE* has a relatively small time complexity and scales well on large networks.

## 5 CONCLUSION

In this paper, we proposed to enhance network structure to improve the performance of existing community detection algorithms. In particular, we put forward two structure enhancement algorithms, namely *RobustECD-GA* and *RobustECD-SE*, taking both robustness and generalization into account. Extensive experimental results demonstrate the superiority of our methods in helping six common community detection algorithms achieve significant performance improvements for both real-world networks and adversarial networks, and further solve the resolution limit in modularity optimization and achieve consensus partitions. We believe this could be a fruitful avenue of future research that address more complex situations like overlapping community in dynamic networks.

## ACKNOWLEDGMENTS

The authors would like to thank all the members in the IVSN Research Group, Zhejiang University of Technology for the valuable discussions about the ideas and technical details presented in this paper. This work was partially supported by the National Natural Science Foundation of China under Grant 61973273, by the Zhejiang Provincial Natural Science Foundation of China under Grant LR19F030001, and by the Hong Kong Research Grants Council under the GRF Grant CityU11200317.

## REFERENCES

- [1] S. H. Strogatz, "Exploring complex networks," *Nature*, vol. 410, no. 6825, p. 268, 2001.
- [2] M. E. Newman, "The structure and function of complex networks," *SIAM Review*, vol. 45, no. 2, pp. 167–256, 2003.
- [3] M. E. J. Newman, "Finding community structure in networks using the eigenvectors of matrices," *Physical Review E*, vol. 74, no. 3, p. 036104, 2006.
- [4] J. Chen, L. Chen, Y. Chen, M. Zhao, S. Yu, Q. Xuan, and X. Yang, "Ga-based q-attack on community detection," *IEEE Transactions on Computational Social Systems*, vol. 6, no. 3, pp. 491–503, 2019.
- [5] V. Fionda and G. Pirro, "Community deception or: How to stop fearing community detection algorithms," *IEEE Transactions on Knowledge and Data Engineering*, vol. 30, no. 4, pp. 660–673, 2017.
- [6] M. Ciglan, M. Laclavík, and K. Nørvåg, "On community detection in real-world networks and the importance of degree assortativity," in *Proceedings of the 19th ACM SIGKDD International Conference on Knowledge Discovery and Data Mining*. ACM, 2013, pp. 1007–1015.
- [7] S. Fortunato and M. Barthelemy, "Resolution limit in community detection," *Proceedings of the National Academy of Sciences*, vol. 104, no. 1, pp. 36–41, 2007.
- [8] L. Lü and T. Zhou, "Link prediction in complex networks: A survey," *Physica A: Statistical Mechanics and its Applications*, vol. 390, no. 6, pp. 1150–1170, 2011.
- [9] M. E. Newman and M. Girvan, "Finding and evaluating community structure in networks," *Physical Review E*, vol. 69, no. 2, p. 026113, 2004.
- [10] L. Danon, A. Diaz-Guilera, J. Duch, and A. Arenas, "Comparing community structure identification," *Journal of Statistical Mechanics: Theory and Experiment*, vol. 2005, no. 09, p. P09008, 2005.
- [11] E.-M. Mohamed, T. Agouti, A. Tikniouine, and M. El Adnani, "A comprehensive literature review on community detection: Approaches and applications," *Procedia Computer Science*, vol. 151, pp. 295–302, 2019.
- [12] V. D. Blondel, J.-L. Guillaume, R. Lambiotte, and E. Lefebvre, "Fast unfolding of communities in large networks," *Journal of Statistical Mechanics: Theory and Experiment*, vol. 2008, no. 10, p. P10008, 2008.
- [13] M. Girvan and M. E. Newman, "Community structure in social and biological networks," *Proceedings of the National Academy of Sciences*, vol. 99, no. 12, pp. 7821–7826, 2002.
- [14] A. Clauset, M. E. Newman, and C. Moore, "Finding community structure in very large networks," *Physical Review E*, vol. 70, no. 6, p. 066111, 2004.
- [15] U. Von Luxburg, "A tutorial on spectral clustering," *Statistics and Computing*, vol. 17, no. 4, pp. 395–416, 2007.
- [16] S. Fortunato, "Community detection in graphs," *Physics Reports*, vol. 486, no. 3-5, pp. 75–174, 2010.
- [17] M. Rosvall and C. T. Bergstrom, "Maps of random walks on complex networks reveal community structure," *Proceedings of the National Academy of Sciences*, vol. 105, no. 4, pp. 1118–1123, 2008.
- [18] V. Zlatić, A. Gabrielli, and G. Caldarelli, "Topologically biased random walk and community finding in networks," *Physical Review E*, vol. 82, no. 6, p. 066109, 2010.
- [19] U. N. Raghavan, R. Albert, and S. Kumara, "Near linear time algorithm to detect community structures in large-scale networks," *Physical Review E*, vol. 76, no. 3, p. 036106, 2007.
- [20] P.-Z. Li, L. Huang, C.-D. Wang, J.-H. Lai, and D. Huang, "Community detection by motif-aware label propagation," *ACM Transactions on Knowledge Discovery from Data (TKDD)*, vol. 14, no. 2, pp. 1–19, 2020.
- [21] L. Huang, H.-Y. Chao, and Q. Xie, "Mumod: A micro-unit connection approach for hybrid-order community detection," in *Proceedings of the AAAI Conference on Artificial Intelligence*, vol. 34, no. 01, 2020, pp. 107–114.
- [22] D. Bo, X. Wang, C. Shi, M. Zhu, E. Lu, and P. Cui, "Structural deep clustering network," in *Proceedings of The Web Conference 2020*, 2020, pp. 1400–1410.
- [23] S. Fan, X. Wang, C. Shi, E. Lu, K. Lin, and B. Wang, "One2multi graph autoencoder for multi-view graph clustering," in *Proceedings of The Web Conference 2020*, 2020, pp. 3070–3076.
- [24] P. De Meo, E. Ferrara, G. Fiumara, and A. Provetti, "Enhancing community detection using a network weighting strategy," *Information Sciences*, vol. 222, pp. 648–668, 2013.
- [25] P. G. Sun, "Weighting links based on edge centrality for community detection," *Physica A: Statistical Mechanics and Its Applications*, vol. 394, pp. 346–357, 2014.
- [26] D. Lai, H. Lu, and C. Nardini, "Enhanced modularity-based community detection by random walk network preprocessing," *Physical Review E*, vol. 81, no. 6, p. 066118, 2010.
- [27] P.-Z. Li, L. Huang, C.-D. Wang, and J.-H. Lai, "Edmot: An edge enhancement approach for motif-aware community detection," in *Proceedings of the 25th ACM SIGKDD International Conference on Knowledge Discovery & Data Mining*, 2019, pp. 479–487.
- [28] A. Lancichinetti and S. Fortunato, "Consensus clustering in complex networks," *Scientific Reports*, vol. 2, p. 336, 2012.
- [29] J. Dahlin and P. Svenson, "Ensemble approaches for improving community detection methods," *Journal of Radioanalytical & Nuclear Chemistry*, vol. 79, no. 3, pp. 191–194, 1997.
- [30] D. He, H. Wang, D. Jin, and B. Liu, "A model framework for the enhancement of community detection in complex networks," *Physica A: Statistical Mechanics and its Applications*, vol. 461, pp. 602–612, 2016.
- [31] C. Szegedy, W. Zaremba, I. Sutskever, J. Bruna, D. Erhan, I. Goodfellow, and R. Fergus, "Intriguing properties of neural networks," Jan. 2014, 2nd International Conference on Learning Representations, ICLR 2014 ; Conference date: 14-04-2014 Through 16-04-2014.
- [32] M. Waniek, T. P. Michalak, M. J. Wooldridge, and T. Rahwan, "Hiding individuals and communities in a social network," *Nature Human Behaviour*, vol. 2, no. 2, p. 139, 2018.
- [33] J. Li, H. Zhang, Z. Han, Y. Rong, H. Cheng, and J. Huang, "Adversarial attack on community detection by hiding individuals," in *Proceedings of The Web Conference 2020*, 2020, pp. 917–927.
- [34] G. Salton and M. J. McGill, *Introduction to Modern Information Retrieval*. mcgraw-hill, 1983.
- [35] P. Jaccard, "Étude comparative de la distribution florale dans une portion des Alpes et des Jura," *Bull Soc Vaudoise Sci Nat*, vol. 37, pp. 547–579, 1901.

- [36] E. Ravasz, A. L. Somera, D. A. Mongru, Z. N. Oltvai, and A.-L. Barabási, "Hierarchical organization of modularity in metabolic networks," *Science*, vol. 297, no. 5586, pp. 1551–1555, 2002.
- [37] L. A. Adamic and E. Adar, "Friends and neighbors on the web," *Social Networks*, vol. 25, no. 3, pp. 211–230, 2003.
- [38] T. Zhou, L. Lü, and Y.-C. Zhang, "Predicting missing links via local information," *The European Physical Journal B*, vol. 71, no. 4, pp. 623–630, 2009.
- [39] M. Zhang and Y. Chen, "Link prediction based on graph neural networks," in *Advances in Neural Information Processing Systems*, 2018, pp. 5165–5175.
- [40] L. Lü, C.-H. Jin, and T. Zhou, "Similarity index based on local paths for link prediction of complex networks," *Physical Review E*, vol. 80, no. 4, p. 046122, 2009.
- [41] S. Brin and L. Page, "The anatomy of a large-scale hypertextual web search engine," *Computer Networks and ISDN Systems*, vol. 30, no. 1-7, pp. 107–117, 1998.
- [42] D. Lin *et al.*, "An information-theoretic definition of similarity," in *International Conference on Machine Learning*, vol. 98, no. 1998. Citeseer, 1998, pp. 296–304.
- [43] W. W. Zachary, "An information flow model for conflict and fission in small groups," *Journal of Anthropological Research*, vol. 33, no. 4, pp. 452–473, 1977.
- [44] M. E. Newman, "Modularity and community structure in networks," *Proceedings of the National Academy of Sciences*, vol. 103, no. 23, pp. 8577–8582, 2006.
- [45] A. Lada and G. Natalie, "The political blogosphere and the 2004 us election," in *Proceedings of the 3rd International Workshop on Link Discovery*, vol. 1, 2005, pp. 36–43.
- [46] J. Yang and J. Leskovec, "Defining and evaluating network communities based on ground-truth," *Knowledge and Information Systems*, vol. 42, no. 1, pp. 181–213, 2015.
- [47] S. Monti, P. Tamayo, J. Mesirov, and T. Golub, "Consensus clustering: a resampling-based method for class discovery and visualization of gene expression microarray data," *Machine Learning*, vol. 52, no. 1-2, pp. 91–118, 2003.
- [48] L. Hubert and P. Arabie, "Comparing partitions," *Journal of Classification*, vol. 2, no. 1, pp. 193–218, 1985.
- [49] P. Pons and M. Latapy, "Computing communities in large networks using random walks," in *International Symposium on Computer and Information Sciences*. Springer, 2005, pp. 284–293.
- [50] A. Grover and J. Leskovec, "node2vec: Scalable feature learning for networks," in *Proceedings of the 22nd ACM SIGKDD International Conference on Knowledge Discovery and Data Mining*. ACM, 2016, pp. 855–864.



**Jiajun Zhou** received the BS degree in automation from the Zhejiang University of Technology, Hangzhou, China, in 2018, where he is currently pursuing the MS degree in control theory and engineering with the College of Information Engineering. His current research interests include graph mining and deep learning, especially for network security.



**Zhi Chen** received the BS and MS degrees in EECS from UC Berkeley, in 2019 and 2020, respectively. He is currently working toward the PhD degree in computer science with the University of Illinois, Urbana-Champaign. At UC Berkeley, he was a research assistant with the Center for Long-Term Cybersecurity from 2019 to 2020, and with BAIR Lab in 2018. His research interests include security and machine learning.



**Min Du** received the PhD degree from the School of Computing, University of Utah in 2018, after completing the bachelor's degree and the master's degree from Beihang University. She is currently a Postdoctoral scholar in EECS Department, UC Berkeley. Her research interests include big data analytics and machine learning security.



**Lihong Chen** received the BS degree from Zhejiang University of Technology, Hangzhou, China, in 2018. She is currently pursuing the MS degree at College of Information Engineering, Zhejiang University of Technology, Hangzhou, China. Her current research interests include social network analysis, evolutionary computing and deep learning.



**Shanqing Yu** received the MS and PhD degrees from the Graduate School of Information, Production and Systems, Waseda University, Japan, and the School of Computer Engineering, in 2008 and 2011 respectively. She is currently a lecturer at the College of Information Engineering, Zhejiang University of Technology. Her research interests cover intelligent computation, data mining and intelligent transport systems.



**Guanrong Chen** (M'89-SM'92-F'97) received the MSc degree in computer science from Sun Yat-sen University, Guangzhou, China in 1981, and the PhD degree in applied mathematics from Texas A&M University, College Station, Texas, in 1987. He has been a chair professor and the founding director of the Centre for Chaos and Complex Networks at the City University of Hong Kong since 2000. Prior to that, he was a tenured full professor with the University of Houston, Texas. He was awarded the 2011 Euler Gold Medal, Russia, and conferred a Honorary Doctorate by the Saint Petersburg State University, Russia in 2011 and by the University of Le Havre, Normandy, France in 2014. He is a member of the Academy of Europe and a fellow of The World Academy of Sciences, and is a Highly Cited Researcher in Engineering as well as in Mathematics according to Thomson Reuters.



**Qi Xuan** (M'18) received the BS and PhD degrees in control theory and engineering from Zhejiang University, Hangzhou, China, in 2003 and 2008, respectively. He was a Post-Doctoral Researcher with the Department of Information Science and Electronic Engineering, Zhejiang University, from 2008 to 2010, and a Research Assistant with the Department of Electronic Engineering, City University of Hong Kong, Hong Kong, in 2010 and 2017. From 2012 to 2014, he was a Post-Doctoral Fellow with the Department of Computer Science, University of California at Davis, CA, USA. He is a member of the IEEE and is currently a Professor with the Institute of Cyberspace Security, College of Information Engineering, Zhejiang University of Technology, Hangzhou, China. His current research interests include network science, graph data mining, cyberspace security, machine learning, and computer vision.

## APPENDIX A

### A.1 Discussion on edge deletion in RobustECD-SE

Similar to *RobustECD-GA*, these two parameters ( $\beta_a, \beta_d$ ) are also available in *RobustECD-SE*. We extensively study the effect of budget parameters in *RobustECD-SE* to support our decision mentioned in Sec. 3.3.1, i.e., we only consider edge addition in *RobustECD-SE* and neglect edge deletion.

Fig. 9 show the relative improvement rate of time in *RobustECD-SE* involving edge deletion. From the comparison results, one can observe that edge deletion brings up extra time consumption in most cases.

Moreover, the impact of edge addition/deletion is shown in Fig. 10, from which one can observe that *RobustECD-SE* with extra edge deletion has the same or worse effect as that with only edge addition in most cases.

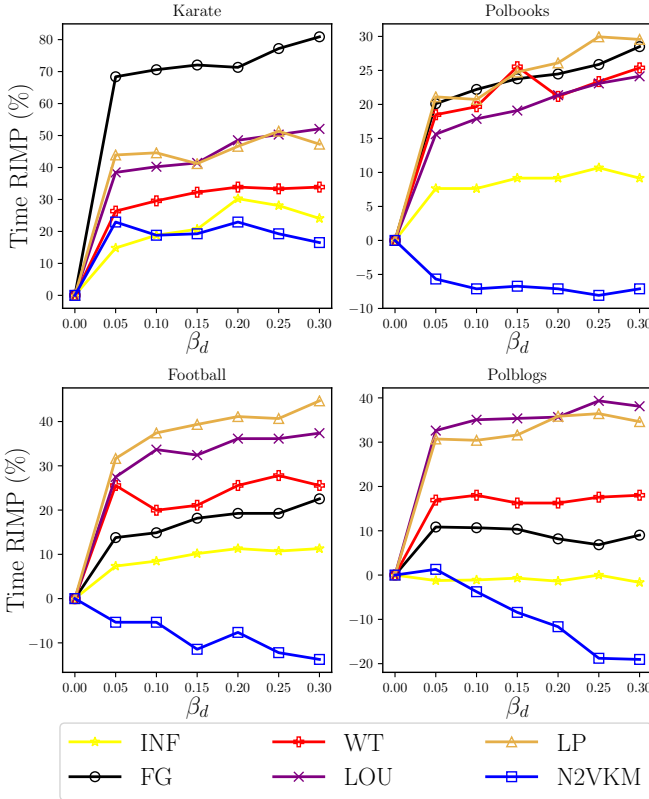


Fig. 9. Extra time consumption of edge deletion in *RobustECD-SE*.

### A.2 Adversarial networks details

Adversarial perturbation is treated as malicious noise, which can be generated via adversarial attack. We consider the following two community deception methods to deploy adversarial attack:

- **Q-Attack** [4]. It is an evolutionary attack strategy based on genetic algorithms, in which the modularity is used to design the fitness function. This strategy deploys attack via negligible network rewiring, which doesn't change the degree of vertices, and achieves the state-of-the-art attack effect.
- **$\mathcal{D}_m$ -Deception via Modularity** [5].  $\mathcal{D}_m$  is a community deception algorithm based on modularity, which

TABLE 8  
Details of attack setup.

Adversarial network	Attack method	Parameter	
		$\mathcal{S}$	$\beta$
Karate(noise)	Q-Attack	LOU	5
Polbooks(noise)	Q-Attack	LOU	20
Football(noise)	$\mathcal{D}_m$	WT	100
Polblogs(noise)	Q-Attack	LOU	100

TABLE 9  
Details of parameter setup in subgraph extraction.

Subgraph of real network	missing data	Parameter	
		$x$	$h$
Amazon-sub	✓	15	4
DBLP-sub	✓	10	3

can hide a target community via intra-community edge deletion and inter-community edge addition.

We generate adversarial networks for all small benchmark networks. Details of attack setup are shown in TABLE 8.

For two large-scale networks, we generate networks with missing data as follows:

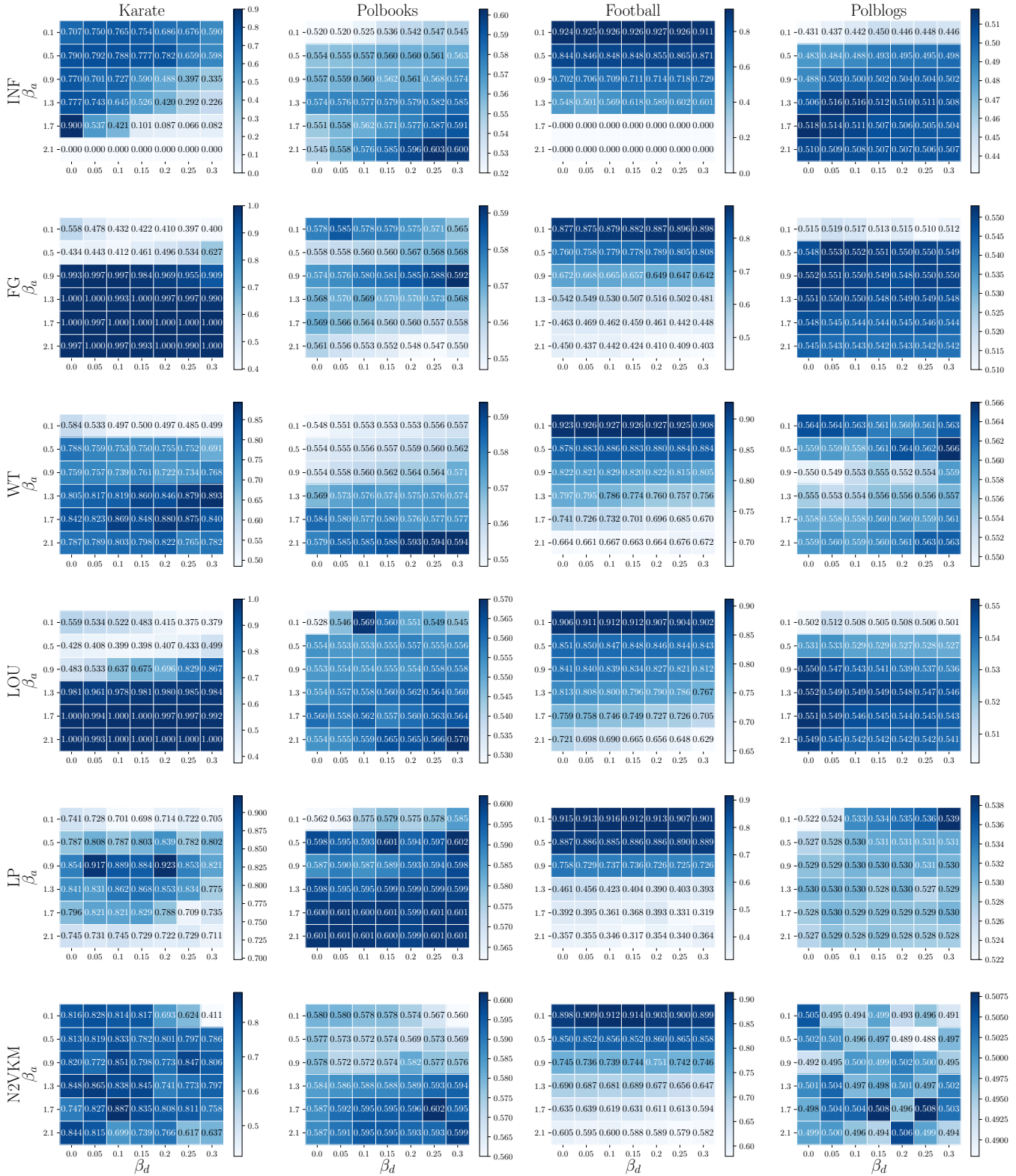
- 1) Select a certain number ( $x$ ) of vertices as community seeds via weighted random sampling, in which the sampling weights are associate with vertex degree;
- 2) Extract  $h$ -hop ego-networks of these seed vertices, and remove those vertices that have multiple community labels;
- 3) Aggregate these ego-networks to form a connected subgraphs.

Details of parameter setup are reported in TABLE 9.

### A.3 Parameter sensitivity of RobustECD-GA

In this subsection, we discuss the impact of key parameters on the performance of *RobustECD-GA*. Fig. 11 shows the parameter sensitivity of *RobustECD-GA*, from which one can see that *RobustECD-GA* performs well in small-scale networks like Karate, Polbooks and Football. In general, *RobustECD-GA* is not strictly sensitive to different parameter settings in most cases, since that the sensitivity curves are smooth over the interval  $[0.04, 0.28]$ . Moreover, with the increase of network scale, like Polblogs, *RobustECD-GA* performs poorly. As a reasonable explanation, *RobustECD-GA* is based on evolutionary computation, which is capable of finding the optimal modification scheme in a small range of solution space. And with the increase of budget, the solution space becomes larger and *RobustECD-GA* is prone to fall into local optimum, leading to a poor performance.

In addition, we also conduct experiments to show the sensitivity with respect to the parameters in genetic algorithm, as shown in Fig. 12. As we can see, *RobustECD-GA* is roughly not sensitive to different parameter settings in most cases. Note that the curves of LP and N2VKM have relatively obvious fluctuation, since that both of the two community detection algorithms have greater randomness.

Fig. 10. The impact of both  $\beta_a$  and  $\beta_d$  in *RobustECD-SE* in term of NMI.

#### A.4 Vertex similarity details

In this subsection, we briefly summarize the definition of similarity indices used in this paper.

- Common Neighbors (CN). It is defined as:

$$\mathcal{H}_{ij} = |\Gamma_i \cap \Gamma_j|, \quad (16)$$

where  $\Gamma_i$  denotes the set of 1-hop neighbors of vertex  $v_i$  and  $|\cdot|$  is the cardinality of the set. It's easy to



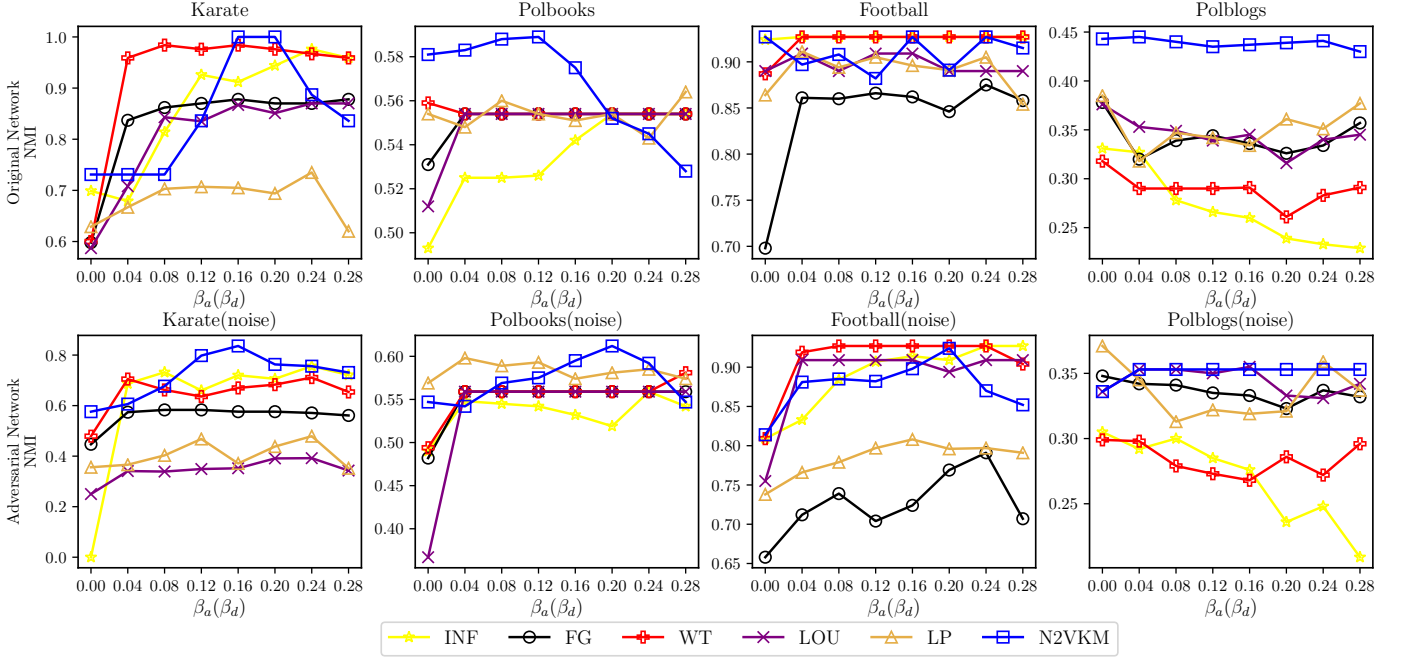


Fig. 11. The impact of modification budgets  $\beta_a$  and  $\beta_d$  on the performance of *RobustECD-GA*.

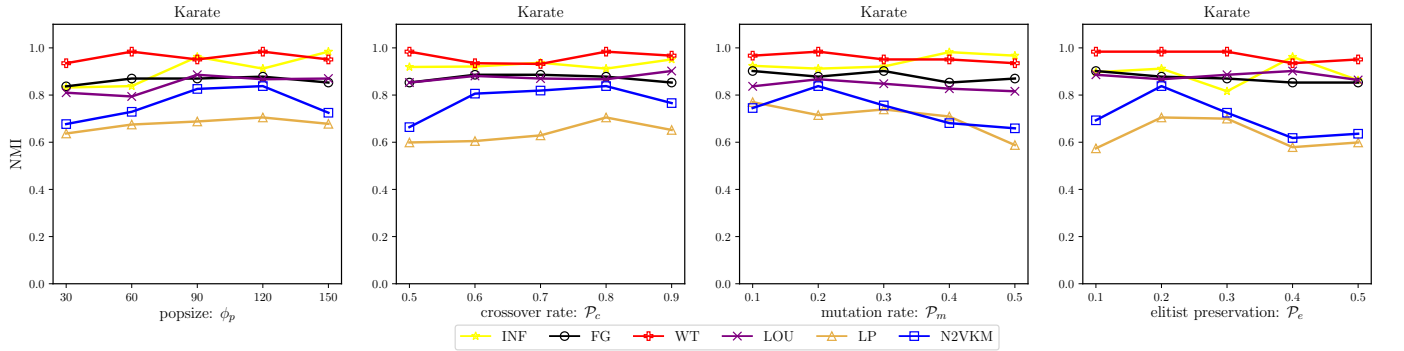


Fig. 12. The impact of GA parameters on the performance of *RobustECD-GA*.

calculate CN by the adjacency matrix  $\mathcal{A}$ , i.e.,  $\mathcal{H}_{ij} = (\mathcal{A}^2)_{ij}$ .

- Salton Index. It is defined as:

$$\mathcal{H}_{ij} = \frac{|\Gamma_i \cap \Gamma_j|}{\sqrt{k_i \times k_j}}, \quad (17)$$

where  $k_i$  denotes the degree of vertex  $v_i$ .

- Jaccard Index. It is defined as:

$$\mathcal{H}_{ij} = \frac{|\Gamma_i \cap \Gamma_j|}{|\Gamma_i \cup \Gamma_j|}. \quad (18)$$

- Hub Promoted Index (HPI). It is defined as:

$$\mathcal{H}_{ij} = \frac{|\Gamma_i \cap \Gamma_j|}{\min\{k_i, k_j\}}. \quad (19)$$

Under this measure, the links adjacent to hubs are likely to be assigned higher scores since the denominator is determined by the lower degree.

- Adamic-Adar Index (AA). It is defined as:

$$\mathcal{H}_{ij} = \sum_{z \in \Gamma_i \cap \Gamma_j} \frac{1}{\log k_z}, \quad (20)$$

where  $z$  is the common neighbor of  $v_i$  and  $v_j$ . The main assumption of this index is that the common neighbors of smaller degrees contribute more to the similarity.

- Resource Allocation Index (RA). It is defined as:

$$\mathcal{H}_{ij} = \sum_{z \in \Gamma_i \cap \Gamma_j} \frac{1}{k(z)}. \quad (21)$$

RA index is similar to AA, but punish more heavily on their common neighbors of high-degree.

- Local Path Index (LP). It is defined as:

$$\mathcal{H}_{ij} = (\mathcal{A}^2)_{ij} + \alpha(\mathcal{A}^3)_{ij}, \quad (22)$$

where  $\alpha$  is a free parameter. LP considers the contribution of third-order neighbors on the basis of Common neighbors (CN), and degenerates to CN when  $\alpha = 0$ .

- RandomWalk with Restart (RWR). Consider a random walker starting from vertex  $v_i$ , who will iteratively moves to a random neighbor with probability  $c$  and return to vertex  $v_i$  with probability  $1 - c$ . Denote

by  $q_{ij}$  the probability this random walker locates at vertex  $v_j$  in the steady state, we have

$$\mathbf{q}_i(t+1) = c\mathbf{P}^T\mathbf{q}_i(t) + (1-c)\mathbf{e}_i, \quad (23)$$

where  $\mathbf{P}$  is the transition matrix with  $\mathbf{P}_{ij} = 1/k_i$  if  $v_i$  and  $v_j$  are connected, and  $\mathbf{P}_{ij} = 0$  otherwise. The solution is straightforward, as

$$\mathbf{q}_i = (1-c) \left( I - c\mathbf{P}^T \right)^{-1} \mathbf{e}_i, \quad (24)$$

The RWR index is thus defined as

$$\mathcal{H}_{ij}^{\text{RWR}} = q_{ij} + q_{ji}, \quad (25)$$

where  $q_{ij}$  is the  $j$ th element of the vector  $\mathbf{q}_i$ .

### A.5 Impact of single similarity index in RobustECD-SE

Fig. 13 and Fig. 14 show the results of all similarity indices (*RobustECD-SE(all)*) and single index (*RobustECD-SE(single)*) in real networks and adversarial networks, respectively. In Karate and Karate(noise) ( $\beta_a \in (1.0, 2.0)$ ), *RobustECD-SE(single)*s with first-order similarity have relatively good performance while those with second-order and high-order similarity have relatively poor performance. Since that the scale of Karate is particularly small and first-order similarity are sufficient to capture structure features, so first-order similarity indices are complementary, second-order and high-order similarity are redundant or even negative in some cases. For Polbooks and Polbooks(noise), *RobustECD-SE(single)* with LP similarity receives the best performance in most cases. The specific definition of Local Path (LP) is  $\mathcal{H} = \mathcal{A}^2 + \alpha\mathcal{A}^3$ , where  $\alpha$  is adjustable parameter. LP considers the contribution of third-order neighbors on the basis of Common neighbors (CN). So other similarity indices are redundant or even negative. For Football and Football(noise) ( $\beta_a \in (0.0, 0.5)$ ), all *RobustECD-SE(single)*s have similarity results and achieve competitive performance against *RobustECD-SE(all)*. Since that Football network has a strong community structures, and single similarity index is sufficient to capture structure features. For polblogs and Polblogs(noise), *RobustECD-SE(single)*s achieve competitive performance against *RobustECD-SE(all)* except for those with Jaccard, Salton and high-order similarity, which turn out to be redundant.

### A.6 Impact of combination of similarity indices in RobustECD-SE

Combined with the conclusions in Appendix A.5, we further explore how to design proper combinations of similarity indices. Table 10 and Table 11 report the results of several special combinations of similarity indices, from which we come to the following conclusions:

- *RobustECD-SE(combination:4)* obtains competitive results compared to *RobustECD-SE(all)*, i.e., after pruning half of the indices according to the category of similarity, *RobustECD-SE* still performs robustly.
- For very small networks like Karate, the combinations of first-order similarity indices (i.e., *RobustECD-SE(combination:1)*) are sufficient to achieve excellent

performance while the combinations of higher-order similarity indices is counterproductive.

- For those networks with strong community structures like Football, different combinations obtain relatively consistent performances, and even a single similarity index is sufficient.

TABLE 10  
Community detection results under different combinations of similarity indices in the real networks.

Dataset	Method	Similarity indices								Community Detection						
		1				2		3		NMI						
		CN	Jaccard	Salton	HPI	AA	RA	LP	RWR	INF	FG	WT	LOU	LP	N2VKM	Avg RIMP
Karate	Original									0.699±0.000	0.598±0.000	0.600±0.000	0.587±0.000	0.689±0.283	0.705±0.175	—
	RobustECD-SE(all)	✓	✓	✓	✓	✓	✓	✓	✓	<b>0.825±0.220</b>	<b>1.000±0.000</b>	0.821±0.088	<b>1.000±0.000</b>	<b>0.847±0.136</b>	<b>0.834±0.114</b>	<b>38.95%</b>
	RobustECD-SE(combination:1)	✓	✓	✓	✓					<b>0.874±0.241</b>	<b>0.997±0.023</b>	<b>0.825±0.099</b>	0.933±0.138	<b>0.839±0.144</b>	<b>0.855±0.109</b>	<b>38.54%</b>
	RobustECD-SE(combination:2)					✓	✓			0.379±0.218	0.974±0.060	0.767±0.120	0.913±0.152	0.771±0.131	0.571±0.263	15.56%
	RobustECD-SE(combination:3)							✓	✓	0.341±0.191	0.942±0.099	0.784±0.144	0.899±0.119	0.729±0.125	0.112±0.190	1.97%
	RobustECD-SE(combination:4)				✓	✓			✓	0.730±0.227	<b>0.997±0.023</b>	<b>0.855±0.119</b>	<b>0.975±0.080</b>	0.809±0.140	0.829±0.111	35.79%
RobustECD-SE(single)				✓				✓	<b>0.825±0.255</b>	0.967±0.065	0.797±0.120	0.821±0.152	0.799±0.136	0.833±0.119	31.09%	
Polbooks	Original									0.493±0.000	0.531±0.000	0.559±0.000	0.512±0.000	0.554±0.025	0.556±0.017	—
	RobustECD-SE(all)	✓	✓	✓	✓	✓	✓	✓	✓	<b>0.574±0.014</b>	<b>0.569±0.001</b>	<b>0.586±0.017</b>	0.560±0.011	<b>0.598±0.009</b>	<b>0.589±0.009</b>	<b>8.61%</b>
	RobustECD-SE(combination:1)	✓	✓	✓	✓					0.561±0.014	0.558±0.014	0.581±0.016	0.556±0.009	0.592±0.014	0.588±0.007	7.34%
	RobustECD-SE(combination:2)					✓	✓			0.562±0.018	0.568±0.007	0.584±0.021	0.561±0.018	0.594±0.013	0.582±0.021	7.82%
	RobustECD-SE(combination:3)							✓	✓	<b>0.577±0.016</b>	<b>0.576±0.014</b>	0.579±0.015	<b>0.571±0.013</b>	<b>0.604±0.017</b>	0.589±0.004	<b>9.26%</b>
	RobustECD-SE(combination:4)				✓	✓			✓	0.572±0.011	0.566±0.010	<b>0.588±0.022</b>	<b>0.563±0.012</b>	0.591±0.015	<b>0.591±0.014</b>	8.46%
RobustECD-SE(single)				✓				✓	0.562±0.016	0.551±0.025	0.575±0.018	0.560±0.019	0.586±0.020	0.589±0.013	6.95%	
Football	Original									0.924±0.000	0.698±0.000	0.887±0.000	0.890±0.000	0.888±0.037	0.912±0.012	—
	RobustECD-SE(all)	✓	✓	✓	✓	✓	✓	✓	✓	<b>0.924±0.000</b>	<b>0.877±0.021</b>	<b>0.923±0.009</b>	<b>0.906±0.014</b>	<b>0.915±0.018</b>	<b>0.898±0.021</b>	<b>5.50%</b>
	RobustECD-SE(combination:1)	✓	✓	✓	✓					<b>0.925±0.001</b>	<b>0.869±0.023</b>	<b>0.920±0.009</b>	0.902±0.015	0.908±0.019	0.894±0.017	4.99%
	RobustECD-SE(combination:2)					✓	✓			0.924±0.001	0.860±0.026	0.918±0.012	0.898±0.019	0.913±0.016	0.890±0.017	4.67%
	RobustECD-SE(combination:3)							✓	✓	0.924±0.001	0.857±0.028	0.916±0.014	<b>0.908±0.019</b>	0.910±0.015	<b>0.899±0.017</b>	4.85%
	RobustECD-SE(combination:4)				✓	✓			✓	0.924±0.001	0.867±0.021	0.918±0.009	0.903±0.017	<b>0.914±0.019</b>	<b>0.892±0.021</b>	4.98%
RobustECD-SE(single)				✓				✓	0.924±0.001	0.864±0.030	0.912±0.015	0.903±0.019	0.911±0.014	<b>0.908±0.017</b>	<b>5.04%</b>	
Polblogs	Original									0.330±0.001	0.378±0.000	0.318±0.000	0.376±0.000	0.375±0.053	0.458±0.067	—
	RobustECD-SE(all)	✓	✓	✓	✓	✓	✓	✓	✓	0.517±0.007	<b>0.551±0.006</b>	0.556±0.009	<b>0.551±0.005</b>	0.529±0.007	<b>0.499±0.006</b>	<b>45.64%</b>
	RobustECD-SE(combination:1)	✓	✓	✓	✓					0.501±0.006	0.544±0.005	0.540±0.007	0.518±0.020	0.522±0.004	0.496±0.003	41.80%
	RobustECD-SE(combination:2)					✓	✓			0.514±0.011	<b>0.555±0.009</b>	<b>0.559±0.009</b>	<b>0.555±0.008</b>	<b>0.531±0.007</b>	0.486±0.012	45.61%
	RobustECD-SE(combination:3)							✓	✓	<b>0.525±0.006</b>	0.548±0.007	<b>0.560±0.011</b>	0.549±0.006	<b>0.532±0.007</b>	<b>0.498±0.007</b>	<b>46.13%</b>
	RobustECD-SE(combination:4)				✓	✓			✓	<b>0.523±0.008</b>	0.548±0.009	0.534±0.012	0.546±0.008	0.526±0.007	0.453±0.005	42.63%
RobustECD-SE(single)				✓				✓	0.521±0.010	0.547±0.009	0.537±0.038	0.549±0.008	0.521±0.013	0.457±0.007	42.70%	

TABLE 11  
Community detection results under different combinations of similarity indices in the adversarial networks.

Dataset	Method	Similarity indices								Community Detection						
		1				2		3		NMI						
		CN	Jaccard	Salton	HPI	AA	RA	LP	RWR	INF	FG	WT	LOU	LP	N2VKM	Avg RIMP
Karate (noise)	Original									0.699±0.000	0.598±0.000	0.600±0.000	0.587±0.000	0.689±0.283	0.705±0.175	63.90%
	Attack									0.000±0.000	0.447±0.000	0.487±0.000	0.250±0.000	0.475±0.337	0.399±0.231	—
	RobustECD-SE(all)	✓	✓	✓	✓	✓	✓	✓	✓	0.425±0.336	<b>0.709±0.218</b>	0.576±0.075	0.484±0.173	<b>0.828±0.197</b>	<b>0.529±0.340</b>	53.31%
	RobustECD-SE(combination:1)	✓	✓	✓	✓					0.594±0.212	<b>0.844±0.179</b>	<b>0.702±0.151</b>	<b>0.598±0.121</b>	<b>0.828±0.106</b>	<b>0.744±0.165</b>	<b>82.06%</b>
	RobustECD-SE(combination:2)					✓	✓			0.052±0.083	0.343±0.142	0.542±0.128	0.324±0.134	0.573±0.160	0.063±0.123	-6.79%
	RobustECD-SE(combination:3)							✓	✓	0.000±0.000	0.532±0.173	0.600±0.140	0.465±0.144	0.621±0.137	0.039±0.112	11.46%
RobustECD-SE(combination:4)				✓	✓			✓	<b>0.608±0.266</b>	0.617±0.259	0.594±0.119	0.411±0.170	0.781±0.181	0.264±0.308	35.96%	
RobustECD-SE(single)				✓				✓	<b>0.628±0.319</b>	0.657±0.618	<b>0.707±0.173</b>	<b>0.579±0.155</b>	0.689±0.155	0.445±0.301	<b>57.19%</b>	
Polbooks (noise)	Original									0.493±0.000	0.531±0.000	0.559±0.000	0.512±0.000	0.554±0.025	0.556±0.017	26.69%
	Attack									0.418±0.004	0.482±0.000	0.393±0.000	0.343±0.000	0.461±0.030	0.462±0.012	—
	RobustECD-SE(all)	✓	✓	✓	✓	✓	✓	✓	✓	<b>0.590±0.014</b>	<b>0.565±0.012</b>	<b>0.599±0.008</b>	0.564±0.010	<b>0.599±0.008</b>	<b>0.643±0.026</b>	<b>40.72%</b>
	RobustECD-SE(combination:1)	✓	✓	✓	✓					0.587±0.016	0.545±0.005	<b>0.599±0.012</b>	0.562±0.014	0.593±0.014	0.635±0.027	39.31%
	RobustECD-SE(combination:2)					✓	✓			<b>0.590±0.016</b>	0.560±0.015	0.593±0.008	0.576±0.016	0.593±0.016	0.595±0.062	38.93%
	RobustECD-SE(combination:3)							✓	✓	<b>0.594±0.013</b>	<b>0.586±0.018</b>	0.590±0.018	<b>0.578±0.018</b>	<b>0.599±0.010</b>	0.632±0.037	<b>41.51%</b>
RobustECD-SE(combination:4)				✓	✓			✓	0.587±0.015	0.554±0.013	0.591±0.008	0.565±0.016	0.594±0.015	<b>0.638±0.034</b>	39.57%	
RobustECD-SE(single)				✓				✓	0.580±0.022	0.548±0.009	0.592±0.016	<b>0.578±0.022</b>	0.586±0.019	0.615±0.035	38.64%	
Football (noise)	Original									0.924±0.000	0.698±0.000	0.887±0.000	0.890±0.000	0.888±0.037	0.912±0.012	11.27%
	Attack									0.809±0.000	0.658±0.000	0.809±0.000	0.755±0.000	0.800±0.051	0.838±0.027	—
	RobustECD-SE(all)	✓	✓	✓	✓	✓	✓	✓	✓	0.809±0.000	0.762±0.024	<b>0.909±0.020</b>	<b>0.886±0.014</b>	<b>0.863±0.051</b>	<b>0.862±0.021</b>	<b>9.38%</b>
	RobustECD-SE(combination:1)	✓	✓	✓	✓					0.809±0.001	0.759±0.039	0.906±0.021	0.881±0.018	0.843±0.049	0.857±0.023	8.61%
	RobustECD-SE(combination:2)					✓	✓			0.809±0.004	0.750±0.036	0.898±0.027	0.873±0.031	0.841±0.049	0.839±0.030	7.64%
	RobustECD-SE(combination:3)							✓	✓	0.809±0.000	<b>0.768±0.035</b>	0.905±0.021	<b>0.887±0.019</b>	0.849±0.045	0.852±0.023	8.98%
RobustECD-SE(combination:4)				✓	✓			✓	0.809±0.001	<b>0.768±0.034</b>	<b>0.911±0.014</b>	0.883±0.020	0.857±0.049	<b>0.860±0.023</b>	<b>9.34%</b>	
RobustECD-SE(single)				✓				✓	0.809±0.000	0.767±0.048	0.906±0.021	0.877±0.027	<b>0.863±0.041</b>	<b>0.860±0.031</b>	9.20%	
Polblogs (noise)	Original									0.330±0.001	0.378±0.000	0.318±0.000	0.376±0.000	0.375±0.053	0.458±0.067	8.60%
	Attack									0.303±0.001	0.348±0.000	0.299±0.000	0.336±0.000	0.340±0.061	0.434±0.034	—
	RobustECD-SE(all)	✓	✓	✓	✓	✓	✓	✓	✓	0.444±0.007	0.505±0.007	<b>0.558±0.005</b>	0.493±0.004	<b>0.500±0.005</b>	<b>0.469±0.023</b>	<b>46.69%</b>
	RobustECD-SE(combination:1)	✓	✓	✓	✓					0.444±0.010	<b>0.513±0.007</b>	0.539±0.009	<b>0.495±0.007</b>	0.499±0.005	<b>0.470±0.003</b>	46.10%
	RobustECD-SE(combination:2)					✓	✓			0.426±0.009	0.488±0.007	0.541±0.011	0.479±0.007	0.429±0.006	0.439±0.010	41.70%
	RobustECD-SE(combination:3)							✓	✓	<b>0.453±0.009</b>	0.499±0.007	<b>0.545±0.009</b>	0.487±0.007	0.496±0.006	0.450±0.009	44.95%
RobustECD-SE(combination:4)				✓	✓			✓	<b>0.458±0.009</b>	<b>0.511±0.007</b>	0.536±0.009	<b>0.497±0.007</b>	<b>0.501±0.006</b>	0.453±0.006	<b>46.15%</b>	
RobustECD-SE(single)				✓				✓	0.419±0.009	0.484±0.007	0.529±0.032	0.478±0.008	0.488±0.010	0.431±0.009	39.90%	

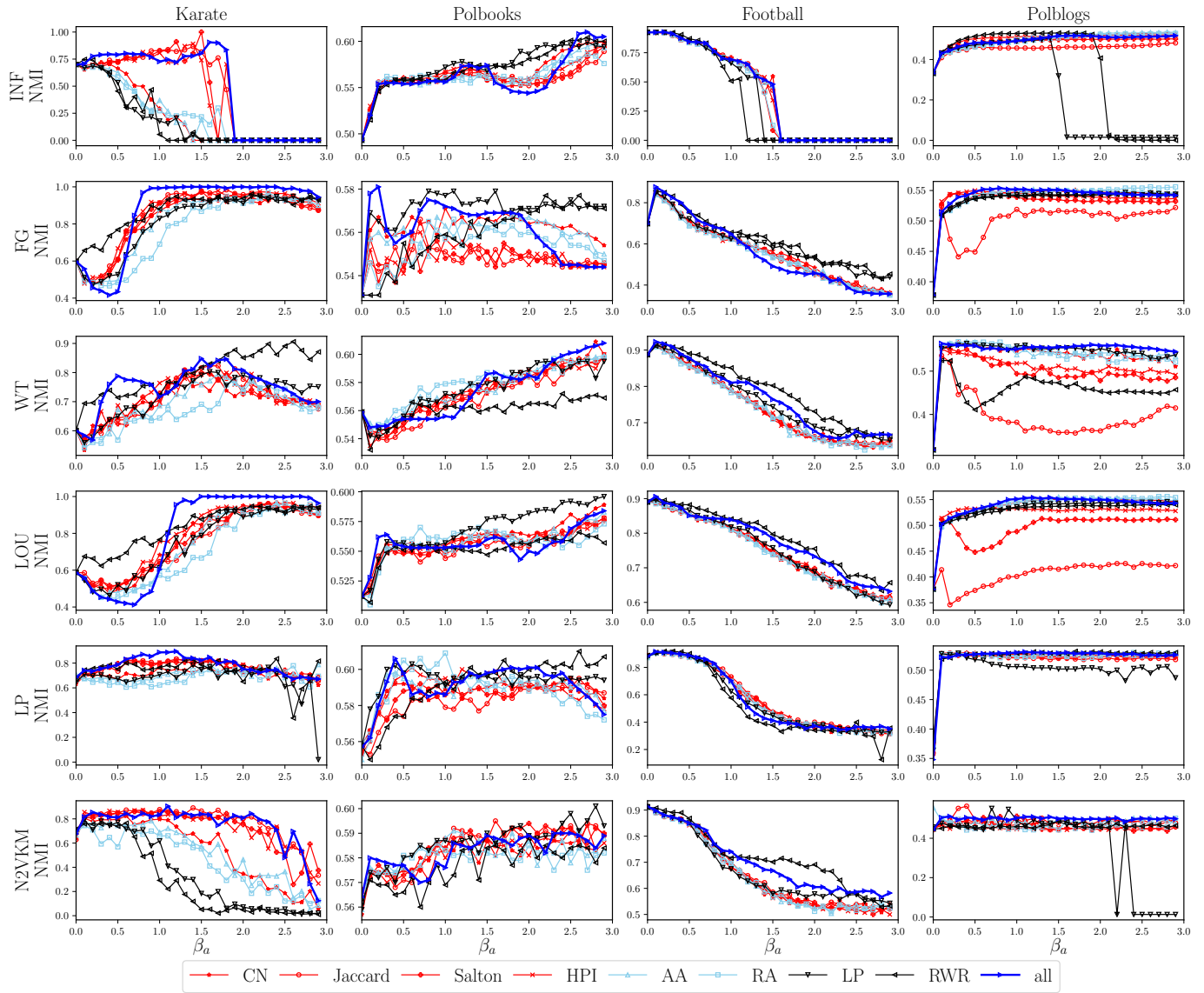


Fig. 13. The impact of single similarity in *RobustECD-SE* for real networks.

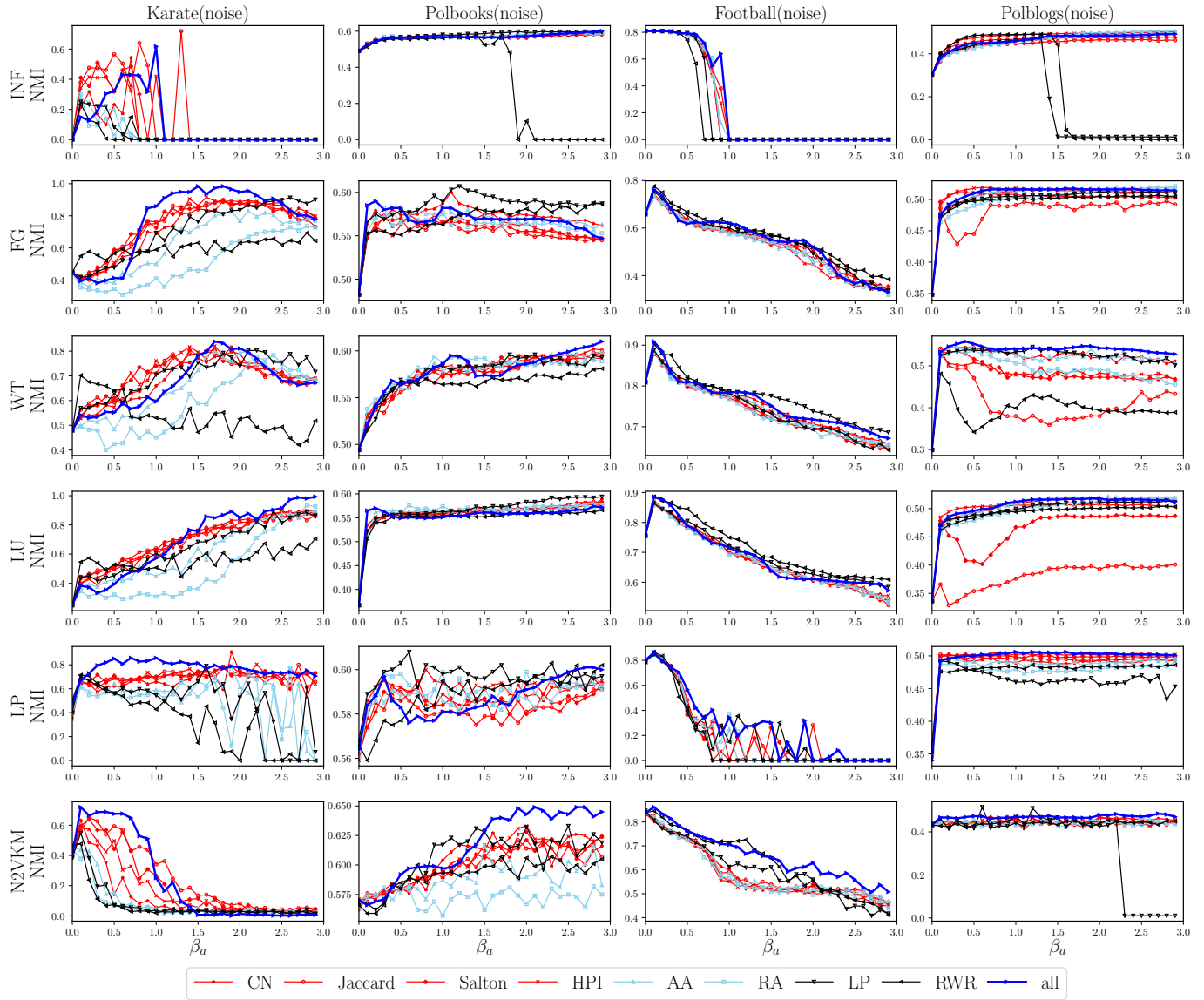


Fig. 14. The impact of single similarity in *RobustECD-SE* for adversarial networks.